
PACED: Distillation at the Frontier of Student Competence

Yuanda Xu*[†] Hejian Sang* Zhengze Zhou*
yuanda@math.princeton.edu hejian@alumni.iastate.edu zz433@cornell.edu

Ran He* Zhipeng Wang
rh2528@columbia.edu zhipeng.wang@alumni.rice.edu

Abstract

Standard LLM distillation wastes compute on two fronts: problems the student has already mastered (near-zero gradients) and problems far beyond its reach (incoherent gradients that erode existing capabilities). We show that this waste is not merely intuitive but structurally inevitable: *the gradient signal-to-noise ratio in distillation provably vanishes at both pass-rate extremes*. This theoretical observation leads to PACED, a framework that concentrates distillation on the *zone of proximal development*—the frontier of a student model’s competence—via a principled pass-rate weight $w(p) = p^\alpha(1-p)^\beta$ derived from the boundary-vanishing structure of distillation gradients.

Key results. **(1) Theory:** We prove that the Beta kernel $w(p) = p^\alpha(1-p)^\beta$ is a leading-order weight family arising from the SNR structure of distillation, and that it is *minimax-robust*—under bounded multiplicative misspecification, worst-case efficiency loss is only $O(\delta^2)$ both pointwise and in aggregate (Theorem 6). **(2) Distillation:** On Qwen3-14B \rightarrow Qwen3-8B with forward KL, PACED achieves +7.5 on MATH-500 and +14.8 on AIME 2025 over the base model, while keeping MMLU forgetting at just 0.2%. **(3) Self-distillation:** On Qwen2.5-Math-7B-Instruct with reverse KL, gains are +9.8 and +13.6, respectively. **(4) Two-stage synergy:** A forward-KL-then-reverse-KL schedule yields the strongest results in our setting, reaching +9.1/ +15.2/ +16.7 on MATH-500/AIME 2024/AIME 2025—supporting a mode-coverage-then-consolidation interpretation of the distillation process. All configurations require only student rollouts to estimate pass rates, need no architectural changes, and are compatible with any KL direction.

1 Introduction

Knowledge distillation trains a student model to imitate a teacher, yet the training budget is spread uniformly across all problems—a striking inefficiency that, as we show formally, is deeply rooted in the gradient structure of distillation itself. On mastered problems ($p \approx 1$), gradients vanish—computation with no learning. On intractable problems ($p \approx 0$), gradients are large but directionally incoherent, actively eroding existing capabilities (French, 1999; Kirkpatrick et al., 2017). We prove that this is not merely anecdotal: *the gradient signal-to-noise ratio (SNR) in distillation provably vanishes at both pass-rate boundaries* (Proposition 2), and under power-law regularity, the Beta kernel $w(p) = p^\alpha(1-p)^\beta$ arises as a leading-order weight family tracking this SNR profile (Proposition 3). This places the zone of proximal development (Vygotsky, 1978)—the frontier between mastery and incompetence—on rigorous footing as a well-motivated training target.

*Equal contribution.

[†]Correspondence to yuanda@math.princeton.edu

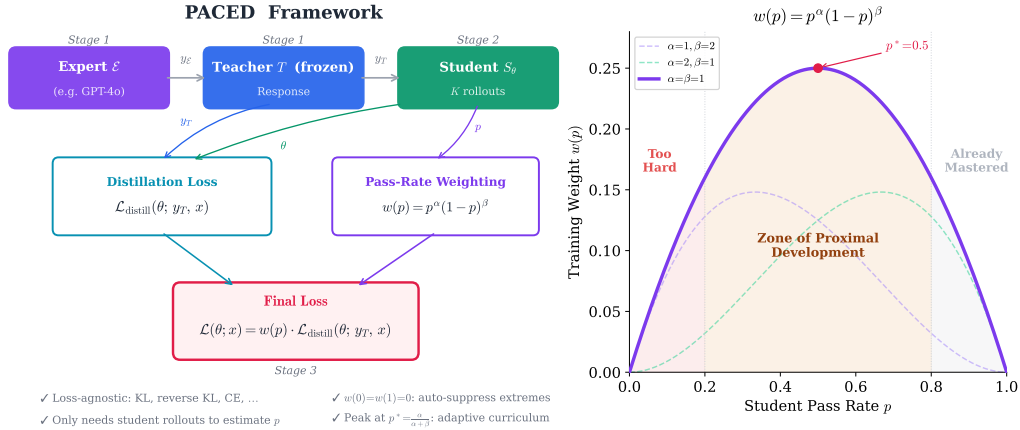


Figure 1: **Overview of PACED.** *Left:* The pipeline—an expert provides reference solutions, and the student learns via a distillation loss weighted by pass rate. *Right:* The Beta-kernel weighting $w(p) = p^\alpha(1 - p)^\beta$ concentrates training on the zone of proximal development, suppressing trivial and intractable problems.

Curriculum learning (Bengio et al., 2009; Kumar et al., 2010) offers a partial answer—train on progressively harder examples—but typically relies on fixed difficulty annotations or predetermined schedules. In distillation, difficulty is not a static property of a problem; it depends on who is solving it and when. A problem that stumps the student in epoch 1 may become tractable by epoch 5.

We propose **Proficiency-Adaptive Competence Enhanced Distillation (PACED)**, a framework that automatically steers distillation toward *the problems where learning actually happens*. The framework is loss-agnostic, architecture-agnostic, and requires only student rollouts. We validate it across two cleanly separated settings: **Distillation** (Qwen3-14B \rightarrow Qwen3-8B, forward KL) and **Self-distillation** (Qwen2.5-Math-7B-Instruct, reverse KL), achieving large gains on reasoning benchmarks (Yu et al., 2025) with near-zero forgetting on MMLU (Hendrycks et al., 2021a). Our contributions are:

1. **A theoretically derived curriculum** (not a heuristic): the Beta-kernel weight $w(p) = p^\alpha(1 - p)^\beta$ emerges as a leading-order family from the boundary-vanishing structure of distillation gradients, rather than from ad-hoc design. The default $w(p) = p(1 - p)$ requires **zero hyperparameter tuning**.
2. **Minimax robustness guarantee**: even when the true gradient SNR deviates from the Beta model by a multiplicative factor $e^{\pm\delta}$, worst-case efficiency loss is only $O(\delta^2)$ —both pointwise and in aggregate (Theorem 6). For $\delta \leq 0.3$ (SNR² within 35%), efficiency exceeds 91%.
3. **Simultaneous plasticity and stability**: PACED delivers +7.5 (MATH-500) and +14.8 (AIME 2025) in the distillation track, and +9.8/ +13.6 in self-distillation—while keeping MMLU forgetting at 0.2% and 0.6%, respectively. A two-stage schedule (forward KL \rightarrow reverse KL) pushes gains to +9.1/ +15.2/ +16.7.
4. **A unifying view of KL directions in distillation**: the dual-track design reveals that forward KL (mode coverage) and reverse KL (mode consolidation) are complementary stages of a single distillation process, not competing alternatives.

An overview appears in Figure 1.

2 Related Work

Knowledge Distillation. The idea of training a smaller model to mimic a larger one dates to Hinton et al. (2015), who showed that the “soft” distribution over classes carries richer information than hard labels alone. Since then, the field has explored sequence-level distillation (Kim and Rush, 2016),

reverse KL objectives (Gu et al., 2024; Agarwal et al., 2024), distribution-aligned methods (Yan et al., 2026; Boizard et al., 2024), and regression-based approaches (Ba and Caruana, 2014; Kim et al., 2021; Wang et al., 2020). A common thread runs through this work: all samples are treated alike. Our contribution is to break this symmetry, letting the student’s own competence determine where training effort flows—regardless of the underlying loss function.

Curriculum Learning. Bengio et al. (2009) articulated the principle that models benefit from seeing easier examples first. Self-paced learning (Kumar et al., 2010) and automated curriculum design (Graves et al., 2017) extended this intuition in various directions. However, existing approaches typically rely on fixed difficulty annotations or predetermined schedules. We propose a finer-grained, fully automatic alternative: a continuous Beta-kernel weight (Section 3.3) derived from gradient-efficiency maximization, which adapts smoothly as the student’s competence evolves—no manual thresholds or scheduling required.

Sample Reweighting. Importance sampling can accelerate SGD by weighting each sample proportionally to its gradient norm (Katharopoulos and Fleuret, 2018), while meta-learning approaches learn per-sample weights end-to-end (Ren et al., 2018). Both demonstrate that non-uniform weighting improves training, but differ from our setting in several ways: the former requires per-sample gradient norms (expensive for LLMs) and the latter requires a clean held-out set plus bi-level optimization; more fundamentally, both target supervised learning and do not address catastrophic forgetting. Our Beta-kernel weight is a closed-form function of the pass rate alone, theoretically grounded in the SNR structure of distillation gradients, and simultaneously serves both learning efficiency and forgetting prevention by suppressing the boundary samples most responsible for capability degradation. In the RL setting, ACE (Xu et al., 2025) introduces per-rollout confidence-based penalty modulation within GRPO/DAPO, targeting overconfident errors rather than uniformly penalizing all incorrect rollouts. While ACE operates at the *rollout level* within RL training, PACED operates at the *problem level* within distillation; the two are complementary.

On-Policy Distillation and Self-Distillation. GKD (Agarwal et al., 2024) trains the student on its own samples rather than the teacher’s, narrowing the train-inference gap. SDFT (Shenfeld et al., 2026) takes this further: the same model plays both teacher (with demonstration context) and student (without), keeping the teacher’s distribution close to the base policy and naturally reducing forgetting. OPSDC (Sang et al., 2026) applies on-policy reverse KL self-distillation to compress verbose chain-of-thought reasoning, conditioning the same model on a conciseness instruction to obtain teacher logits. Our framework shares the self-distillation backbone to some extent but is more general in two respects: it is not restricted to self-distillation—we also evaluate with a larger same-family teacher (Qwen3-14B → Qwen3-8B)—and the pass-rate weighting is loss-agnostic, applicable to both forward and reverse KL (and potentially other objectives). Rather than compressing reasoning length, pass-rate weighting determines *which* problems to prioritize. Distillation already mitigates forgetting relative to SFT on hard labels, since soft targets preserve richer distributional information (Hinton et al., 2015; Shenfeld et al., 2026); we therefore adopt distillation as the training paradigm and focus on further improving it through principled sample weighting. Accordingly, SFT is not included as a baseline: the distillation-vs-SFT comparison is well established in prior work (Hinton et al., 2015; Kim and Rush, 2016; Gu et al., 2024; Shenfeld et al., 2026), and our contribution is orthogonal—improving *how* distillation allocates its training budget, not whether distillation should be preferred over SFT.

Catastrophic Forgetting. EWC (Kirkpatrick et al., 2017), GEM (Lopez-Paz and Ranzato, 2017), and OGD (Farajtabar et al., 2020) all combat forgetting by constraining parameter updates. Our approach takes a different path: rather than adding explicit regularization, we prevent forgetting through curriculum design, filtering out the training signals most likely to cause harm before they ever reach the optimizer.

2.1 Method Positioning Summary

Table 1: **Method-feature comparison.** ✓ = primary design characteristic.

Feature	Self-Dist.	AdaRFT	AdaKD	AKL	PACED
Adaptive weighting / curriculum		✓	✓	✓	✓
Student-side competence signal		✓			✓
Implicit forgetting reduction	✓				✓
Loss-agnostic			✓		✓
Theoretically grounded				✓	✓

3 Methodology

PACED rests on a single core idea: a weighting scheme that directs distillation toward the problems where it can do the most good (Section 3.3).

3.1 Problem Setup

We use two disjoint training splits: $\mathcal{D}^{\text{dist}}$ for distillation and $\mathcal{D}^{\text{self}}$ for self-distillation. Let T denote the frozen teacher model and S_θ the student model. In distillation, T is a larger same-family model (Qwen3-14B) and S_θ is Qwen3-8B. In self-distillation, T is a frozen copy of Qwen2.5-Math-7B-Instruct and S_θ is the trainable copy. In both settings, T is fixed while θ is updated.

For each prompt x , we sample K rollouts from the student and compute the **pass rate**:

$$p(x; \theta) = \frac{1}{K} \sum_{k=1}^K \mathbb{1}[\text{correct}(y_S^{(k)}, x)], \quad y_S^{(k)} \sim \pi_\theta(\cdot | x) \quad (1)$$

The pass rate $p \in [0, 1]$ measures the student’s current competence on problem x .

3.2 Reference Response Generation

The most capable frontier models—gpt-oss-120b (OpenAI, 2025), Claude, Gemini—are accessible only through black-box APIs. We obtain expert solutions via the API and use them as reference responses for distillation. Specifically, a frozen teacher model T generates a complete solution conditioned on the problem and the expert solution:

$$y_T \sim P_T(y | x, y_E) \quad (2)$$

Because the teacher re-expresses the expert’s reasoning in its own distributional voice, the reference response is naturally within the model family’s expressive range—a target the student can realistically aspire to. This design also turns black-box expert supervision into white-box distillation signals: once transferred into same-family teacher outputs, we can train on full token-level logits (forward/reverse KL), rather than being limited to hard-label SFT on API text alone.

Figure 2 shows a concrete prompt template used in our pipeline: the student sees only the original problem, while the teacher additionally receives the expert solution as context.

Teacher configuration. To keep the story clean, we bind one KL direction to each setting: distillation (Qwen3-14B \rightarrow Qwen3-8B) uses forward KL, and self-distillation (Qwen2.5-Math-7B-Instruct) uses reverse KL. This pairing reflects their roles: forward KL favors broad teacher-mode coverage when student–teacher capacity differs, while reverse KL favors compact, high-confidence modes when teacher and student are near-policy.

3.3 Pass-Rate Weighting

Motivation. Not all training problems contribute equally. At one extreme ($p \approx 0$), the student cannot solve the problem at all; logit gradients are large but point in near-random directions across prompts, offering high variance and little useful signal. At the other extreme ($p \approx 1$), the student already matches the teacher; gradients are negligibly small. In practice a substantial fraction of problems falls

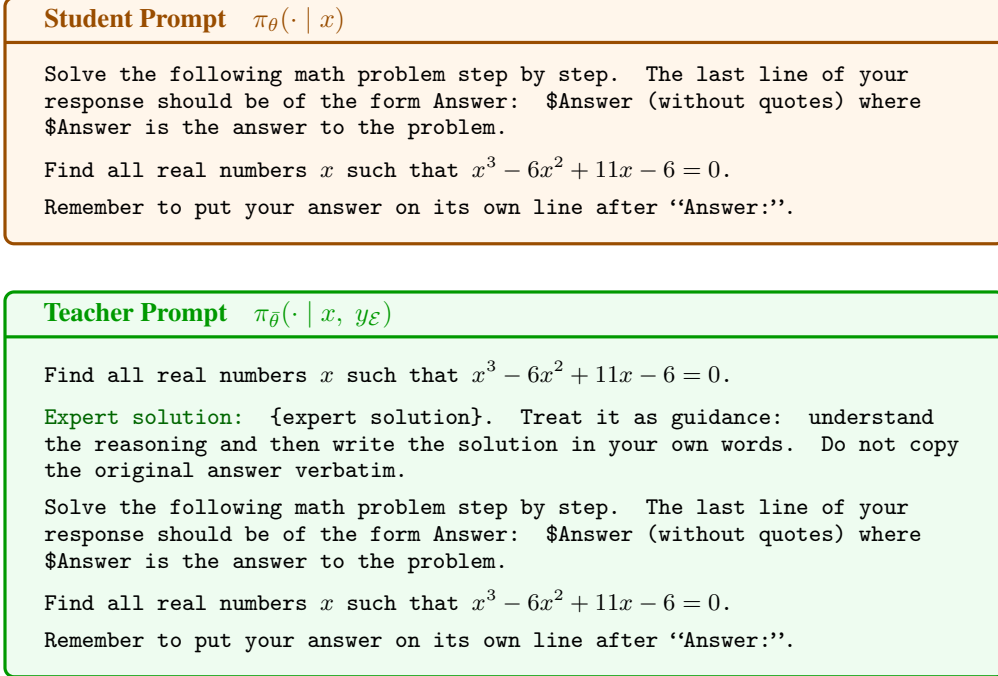


Figure 2: **Prompt example for student and teacher policies.** Both policies share the same model family but differ in conditioning context. The teacher receives the expert solution $y_{\mathcal{E}}$ as additional context, while the student receives only the original problem. This contextual asymmetry enables black-box expert guidance to be transferred into white-box teacher logits for distillation.

into these uninformative extremes—e.g., with Qwen3-8B on DAPO, roughly 49% of problems have $p < 0.2$ or $p > 0.8$ (the exact proportion depends on the model and dataset). The richest—highest signal-to-noise ratio—gradient signal concentrates at *intermediate* difficulty, where the student is partially competent and each update carries genuine information. This raises a natural question: *what is the principled weight function that exploits this structure?*

Theoretical answer. In distillation, the gradient signal-to-noise ratio (SNR) vanishes at both boundaries: at $p \rightarrow 0$ (gradient incoherence) and $p \rightarrow 1$ (alignment at mastery; Proposition 2). Under power-law regularity at the boundaries (Assumption 3(b)), any such SNR profile decomposes as $p^{\alpha'}(1-p)^{\beta'}$ with bounded remainder (Proposition 3). The leading-order, maximum-parsimony weight family is therefore the Beta kernel:

$$w(p) = p^{\alpha}(1-p)^{\beta} \tag{3}$$

with peak at $p^* = \alpha/(\alpha + \beta)$. The default choice $\alpha = \beta = 1$ gives $w(p) = p(1-p)$, which is symmetric around $p^* = 0.5$, zero at the boundaries, and equals the inverse Bernoulli Fisher information (Remark 5). Asymmetric choices ($\alpha \neq \beta$) shift the peak to prioritize harder or easier problems. This form is minimax-robust: even when the true SNR profile deviates from the Beta model by a multiplicative factor $e^{\pm\delta}$, the worst-case efficiency loss is only $O(\delta^2)$ (Theorem 6). See Appendix A.4 for the full derivation.

Crucially, having a realistic target is what makes pass-rate weighting meaningful: because y_T is attainable (Section 3.2), the student’s pass rate p genuinely reflects a learnable gap rather than an architectural mismatch, and the Beta kernel can reliably direct effort to where that gap is most productive.

Algorithm 1 PACED: Competence-Aware Distillation with Pass-Rate Weighting

Require: Prompt dataset \mathcal{D} , expert \mathcal{E} , teacher T , student S_θ ($T = S_\theta$ initially), distillation loss $\mathcal{L}_{\text{distill}}$, weight exponents (α, β) (default $\alpha=\beta=1$), rollouts K

- 1: **// Stage 1: Reference Response Generation**
- 2: **for** each prompt $x \in \mathcal{D}$ **do**
- 3: $y_{\mathcal{E}} \leftarrow \mathcal{E}(x)$ {Expert rollout (e.g., gpt-oss-120b solution)}
- 4: $y_T \leftarrow T(\cdot \mid x, y_{\mathcal{E}})$ {Teacher regeneration conditioned on expert solution}
- 5: **end for**
- 6: **// Stage 2: One-shot pass-rate estimation (paper setting)**
- 7: **for** each prompt $x_i \in \mathcal{D}$ **do**
- 8: Sample $\{y_{S,i}^{(k)}\}_{k=1}^K \sim \pi_\theta(\cdot \mid x_i)$
- 9: $p_i \leftarrow \frac{1}{K} \sum_k \mathbb{1}[\text{correct}(y_{S,i}^{(k)}, x_i)]$
- 10: $w_i \leftarrow p_i^\alpha (1 - p_i)^\beta$ {Default: $w_i = p_i(1 - p_i)$ }
- 11: **end for**
- 12: $\tilde{w}_i \leftarrow w_i / \bar{w}$ for all i {Normalize to unit mean and keep fixed during training}
- 13: **// Stage 3: Weighted Distillation**
- 14: **for** each training iteration **do**
- 15: **for** each prompt $x_i \in \mathcal{D}$ **do**
- 16: $\mathcal{L}(x_i) \leftarrow \tilde{w}_i \cdot \mathcal{L}_{\text{distill}}(\theta; y_{T,i}, x_i)$
- 17: **end for**
- 18: Update θ via gradient descent on $\frac{1}{N} \sum_i \mathcal{L}(x_i)$
- 19: **end for**
- 20: **// Optional extension (not used in this paper):** periodically recompute $\{p_i, \tilde{w}_i\}$

3.4 Overall Algorithm

Putting the pieces together: each problem’s contribution to the loss is scaled by how informative it is for the student right now:

$$\mathcal{L}(\theta; x) = w(p) \cdot \mathcal{L}_{\text{distill}}(\theta; y_T, x) \quad (4)$$

where $p = p(x; \theta)$, $w(p) = p(1 - p)$ by default, and $\mathcal{L}_{\text{distill}}$ is chosen by training setting. We naturally use the two KL directions as follows:

- **Distillation track (Qwen3): Forward KL** along the teacher sequence y_T : $\sum_t D_{KL}(p_T(\cdot \mid y_{T,<t}) \parallel p_S(\cdot \mid y_{T,<t}))$.
- **Self-distillation track (Qwen2.5): Reverse KL** along a student sequence $y_S \sim \pi_\theta(\cdot \mid x)$: $\sum_t D_{KL}(p_S(\cdot \mid y_{S,<t}) \parallel p_T(\cdot \mid y_{S,<t}))$.

$$\mathcal{L}(\theta) = \frac{1}{N} \sum_{i=1}^N \mathcal{L}(\theta; x_i) \quad (5)$$

Iterative Refinement. The curriculum is not static: as training reshapes the student’s abilities, pass rates shift. *In the single-loss experiments reported in this paper, we estimate pass rates once before optimization and keep the resulting weights fixed throughout training* (single-pass weighting). The only exception is the two-stage schedule in Section 4.3, where pass rates are recomputed once at the stage boundary before Stage 2 begins. In longer schedules, one can optionally recompute pass rates at regular intervals so the weighting tracks evolving competence, migrating problems from the “too hard” tail into the fertile middle ground and eventually out the “mastered” side.

3.5 Theoretical Guarantees

We provide theoretical justification for Beta-kernel weighting. Key results are summarized below; full proofs, assumptions, and regime distinctions appear in Appendix A.

Key Results at a Glance

- **Structural characterization:** Distillation gradient SNR vanishes at both boundaries (Prop 2); with power-law regularity, any such profile decomposes as $p^{a'}(1-p)^{b'}$ with bounded r (Prop 3), yielding the Beta kernel as the leading-order weight family
- **Minimax robustness (Main Theorem):** Under bounded misspecification $|r(p)| \leq \delta$, the Beta kernel is minimax-optimal for the low-SNR approximation, with worst-case efficiency $\text{sech}^2(\delta) \geq 1 - \delta^2$, both pointwise and in aggregate (Thm 6)
- **Batch-level variance reduction:** $R < 1$ when $-\text{Cov}(\tilde{w}^2, s^2) > \text{Var}(\tilde{w}) \mathbb{E}[s^2]$ (Prop 7)
- **Exponent selection:** $(\alpha^* + 1)/(\alpha^* + \beta^* + 2) = \bar{p}_Z$, $\alpha^* + \beta^* = \bar{p}_Z(1 - \bar{p}_Z)/\text{Var}_Z(p) - 3$ (Prop 11)

Result 1: Structural characterization of the Beta kernel family (Propositions 2–3). In distillation, the gradient signal-to-noise ratio (SNR) vanishes at both pass-rate extremes: as $p \rightarrow 0$, gradients from different intractable problems become directionally incoherent, so $\text{SNR}(p) \rightarrow 0$; as $p \rightarrow 1$, the student matches the teacher and the gradient signal vanishes. Under power-law boundary regularity (Assumption 3(b)), Proposition 3 shows that *any* such SNR profile decomposes as $\text{SNR}^2(p) = p^{a'}(1-p)^{b'} \cdot e^{r(p)}$ with bounded remainder r . Setting the shape variation of r to zero (maximum parsimony) yields the Beta kernel $p^{a'}(1-p)^{b'}$ as the natural weight family. In other words, the functional form is dictated by boundary structure, not introduced by optimization.

Result 2: Minimax robustness guarantee (Theorem 6, Main Theorem). The Beta kernel is not only a convenient approximation: it is *minimax-optimal at leading order in the low-SNR regime* over the non-parametric uncertainty set $\{\phi : |\log \phi(p)| \leq \delta\}$ induced by bounded remainder r . Concretely, if true SNR^2 deviates from the Beta model by at most a factor $e^{\pm\delta}$, worst-case descent efficiency is $\text{sech}^2(\delta) \geq 1 - \delta^2$, both pointwise (fixed p) and in aggregate (Theorem 6(iii)). For moderate misspecification ($\delta \leq 0.3$, i.e., SNR^2 within 35% of the Beta model), aggregate efficiency exceeds 91%. See Appendix A.4.

Result 3: Batch-level gradient variance reduction (Proposition 7).

The intuition: Non-uniform weighting has two opposing effects on gradient variance:

1. **Bad:** Downweighting some samples reduces the effective batch size, which *increases* variance.
2. **Good:** If we downweight samples that have high gradient variance (noisy gradients), this *decreases* variance.

The resolution: Which force wins? Let σ_{eff}^2 and σ_{unif}^2 denote the gradient variance under Beta-kernel and uniform weighting, respectively. Their ratio admits a revealing decomposition:

$$R = \frac{1 + \underbrace{\text{Var}_P(\tilde{w})}_{\text{penalty from non-uniform weights}} + \underbrace{\frac{\text{Cov}_P(\tilde{w}^2, s^2)}{\mathbb{E}_P[s^2]}}_{\text{coupling between weight and second moment}} - \underbrace{\frac{\|\mathbb{E}_P[\tilde{w}g]\|^2}{\mathbb{E}_P[s^2]}}_{\text{mean-subtraction correction}}}{1 - \frac{\|\mathbb{E}_P[g]\|^2}{\mathbb{E}_P[s^2]}} \quad (6)$$

where \tilde{w} is the normalized weight, g is the per-sample gradient, and $s^2(p) = \mathbb{E}[\|g(p)\|^2]$ is the gradient second moment at pass rate p . In the low-SNR regime—where the mean terms are small relative to $\mathbb{E}_P[s^2]$ —the story simplifies: variance reduction happens when the weight–second-moment covariance is sufficiently negative.

Why Beta kernels win this tug of war: When gradient variance runs hottest at extreme pass rates (Assumption 3(c)), the Beta kernel assigns near-zero weight exactly where s^2 is largest, and concentrates weight where gradients carry real information. This targeted suppression of the noisiest samples can overcome the penalty of non-uniformity, yielding $R < 1$ and faster convergence. Concrete parameter regimes are identified in Appendix A.5.

Result 4: Data-driven exponent selection (Proposition 11).

The concern: The default $\alpha = \beta = 1$ is a reasonable starting point, but can we do better? And can the *theory* tell us the optimal (α, β) from observable quantities, rather than requiring a grid search?

The answer: Yes. The peak location p^* and kernel concentration can be determined by matching the kernel shape to the pass-rate distribution within the zone of proximal development (ZPD). Concretely, define the ZPD as the set of problems with intermediate pass rates: $\mathcal{Z} = \{i : \epsilon \leq p_i \leq 1 - \epsilon\}$ for a cutoff ϵ (e.g., $\epsilon = 1/K$). Then the exponents can be estimated from two empirical moments of the pass-rate distribution restricted to \mathcal{Z} . Since the kernel $w(p) = p^\alpha(1 - p)^\beta$ normalized over $[0, 1]$ yields a $\text{Beta}(\alpha+1, \beta+1)$ density, we apply standard moment matching to this distribution:

$$\frac{\alpha^* + 1}{\alpha^* + \beta^* + 2} = \bar{p}_{\mathcal{Z}}, \quad \alpha^* + \beta^* = \frac{\bar{p}_{\mathcal{Z}}(1 - \bar{p}_{\mathcal{Z}})}{\text{Var}_{\mathcal{Z}}(p)} - 3 \tag{7}$$

where $\bar{p}_{\mathcal{Z}}$ and $\text{Var}_{\mathcal{Z}}(p)$ are the mean and variance of $\{p_i\}_{i \in \mathcal{Z}}$. The kernel peak $p^* = \alpha^*/(\alpha^* + \beta^*)$ is approximately $\bar{p}_{\mathcal{Z}}$ for concentrated distributions. If the informative problems have pass rates concentrated around 0.4 with low variance, the formula prescribes an asymmetric kernel ($\alpha^* < \beta^*$) peaked near $p^* \approx 0.4$; if they are spread broadly, it prescribes a flatter kernel (small $\alpha^* + \beta^*$). The formula requires no gradient computation—only the pass rates already computed for weighting. See Appendix A.6 for the derivation.

Forgetting reduction. Empirically, Beta-kernel weighting substantially reduces catastrophic forgetting by suppressing gradient updates from boundary-pass-rate samples, which tend to carry noisy signals that erode prior capabilities; see Tables 4 and 5 for quantitative results.

4 Experiments

4.1 Experimental Setup

- **External Expert:** gpt-oss-120b (OpenAI, 2025) for initial solution generation.
- **Teacher/Student Models (split by setting):**
 - **Distillation setting:** Qwen3-8B (Qwen Team, 2025) as student, frozen Qwen3-14B as teacher, and **forward KL** as base loss.
 - **Self-distillation setting:** Qwen2.5-Math-7B-Instruct (Yang et al., 2024) with a frozen self-teacher, and **reverse KL** as base loss.

In both settings, the teacher is frozen throughout training.

- **Training data split:** We split DAPO (Yu et al., 2025) into two disjoint partitions, one per setting. This avoids cross-setting leakage and keeps the two narratives (distillation vs self-distillation) independently interpretable.
- **Evaluation:**
 - *Plasticity* (new skill acquisition): mean@8 accuracy on MATH-500 (Hendrycks et al., 2021b), AIME 2024, and AIME 2025 (out-of-distribution generalization). For each problem, we sample 8 responses (temperature 0.6, top- p 0.95) and report mean@8.
 - *Stability* (retention of prior knowledge): MMLU (Hendrycks et al., 2021a).
- **Rollouts:** $K = 8$ rollouts per problem for pass-rate estimation.
- **Pass-rate weight:** Default $w(p) = p(1 - p)$ (i.e., $\alpha = \beta = 1$). In this paper, pass rates are estimated once before optimization; the resulting weights are normalized to unit mean (i.e., $\tilde{w}_i = w_i/\bar{w}$) and then kept fixed during training.
- **Baselines (setting-specific):**
 - **Distillation/Qwen3:** Forward KL (unweighted), Hard Filter Forward KL, AKL, and PACED Forward KL.
 - **Self-distillation/Qwen2.5:** Reverse KL (unweighted), Hard Filter Reverse KL, AKL, and PACED Reverse KL.
 - **AKL (Wu et al., 2025):** An adaptive KL divergence baseline that dynamically adjusts the per-token KL coefficient based on the discrepancy between student and teacher logits. Unlike PACED, which operates at the *problem level* (weighting entire problems

by pass rate), AKL operates at the *token level* (modulating the KL penalty at each decoding step). AKL requires no rollout or pass-rate estimation—the adaptive coefficient is computed from teacher–student logit differences during training. All other hyperparameters (learning rate, batch size, number of epochs) are kept identical to the corresponding unweighted baseline.

4.2 Main Results (Plasticity-Stability Trade-off)

Table 2: Distillation track (Qwen3-14B → Qwen3-8B, forward KL family): reasoning performance (mean@8). ↑ = higher is better.

Method	MATH-500 (↑)	AIME 24 (↑)	AIME 25 (↑)
Base	86.5%	28.7%	20.8%
Forward KL (unweighted)	90.4%	35.9%	29.3%
Hard Filter Forward KL	92.7%	39.5%	33.9%
AKL	91.9%	39.8%	34.1%
PACED Forward KL	94.0%	41.6%	35.6%

Table 3: Self-distillation track (Qwen2.5-Math-7B-Instruct, reverse KL family): reasoning performance (mean@8).

Method	MATH-500 (↑)	AIME 24 (↑)	AIME 25 (↑)
Base	83.9%	19.6%	11.5%
Reverse KL (unweighted)	90.4%	25.3%	16.9%
Hard Filter Reverse KL	92.0%	28.9%	22.0%
AKL	91.4%	28.2%	21.5%
PACED Reverse KL	93.7%	31.6%	25.1%

f

Table 4: Retention in distillation track (Qwen3 forward KL family): MMLU and forgetting (Δ from base).

Method	MMLU (↑)	Forgetting (↓)	Weighting
Base	73.2%	–	–
Forward KL (unweighted)	66.4%	6.8%	None
Hard Filter Forward KL	70.7%	2.5%	Hard
AKL	68.6%	2.8%	Token-level
PACED Forward KL	73.0%	0.2%	Beta

Reasoning (Tables 2 and 3). With the split-track protocol, the pattern is consistent in both settings. In the distillation track (Qwen3, forward KL family), PACED improves MATH-500 from 90.4% to 94.0% and boosts AIME 2024/2025 by +5.7/ + 6.3 points over unweighted forward KL. In the self-distillation track (Qwen2.5, reverse KL family), PACED improves MATH-500 from 90.4% to 93.7% and boosts AIME 2024/2025 by +6.3/ + 8.2 points over unweighted reverse KL.

AKL baseline comparison. AKL (Wu et al., 2025) is a strong baseline that also adapts the distillation signal dynamically, but at a fundamentally different granularity: it modulates the KL coefficient *per token* based on teacher–student logit discrepancy, whereas PACED modulates *per problem* based on pass rate. AKL improves over unweighted training, confirming that adaptive weighting is beneficial. However, PACED consistently outperforms AKL on all reasoning benchmarks in both tracks (e.g., +2.1/ + 1.8/ + 1.5 on MATH-500/AIME 24/AIME 25 in distillation; +1.9/ + 2.4/ + 2.6 in self-distillation), with comparable or lower forgetting. The gap reflects a **structural** difference between token-level and problem-level adaptation. AKL adjusts *how much* the student learns from each token within a given problem, but treats all problems equally—an intractable problem ($p \approx 0$) receives the same total training budget as a productive one ($p \approx 0.5$). This means AKL cannot suppress the noisy, high-variance gradients from intractable problems or the redundant gradients from mastered

Table 5: Retention in self-distillation track (Qwen2.5 reverse KL family): MMLU and forgetting (Δ from base).

Method	MMLU (\uparrow)	Forgetting (\downarrow)	Weighting
Base	70.6%	–	–
Reverse KL (unweighted)	68.4%	2.2%	None
Hard Filter Reverse KL	70.1%	0.5%	Hard
AKL	69.8%	0.8%	Token-level
PACED Reverse KL	70.0%	0.6%	Beta

ones; it only rebalances *within* each problem. In contrast, PACED operates at the problem level via a *continuous* Beta kernel $w(p) = p^\alpha(1-p)^\beta$, concentrating the entire training budget on problems where the student has partial competence. Notably, the two approaches are *orthogonal* and could in principle be combined: PACED selects *which* problems to train on, while AKL optimizes *how* to train on each selected problem.

Stability (Tables 4 and 5). Forgetting reduction remains strong after splitting by setting. In distillation, PACED forward KL reduces forgetting from 6.8 to 0.2 points. In self-distillation, reverse-KL-based methods already forget less, and PACED keeps forgetting in the low range (0.6 points) while preserving the largest reasoning gains. AKL reduces forgetting relative to unweighted training—its per-token adaptation implicitly down-weights tokens where the teacher–student gap is extreme—but PACED still achieves lower or comparable forgetting in both tracks. The difference is that AKL cannot suppress entire intractable problems: even with per-token adaptation, passing gradients through a $p \approx 0$ problem injects noise that accumulates across tokens.

4.3 Ablation Studies (Validating Each Component’s Necessity)

4.3.1 Effect of Weight Exponents

Ablations in this section use Qwen3-8B as the primary model.

Table 6: Ablation on pass-rate weight exponents $w(p) = p^\alpha(1-p)^\beta$ using forward KL divergence as the distillation loss (Qwen3-8B).

α	β	MATH-500 (\uparrow)	Forgetting on MMLU (\downarrow)
1	1	94.0%	0.2%
1	2	95.4%	0.9%
2	1	91.5%	1.8%
1	3	94.9%	2.4%
3	1	90.3%	1.7%

Interpretation. The ablation reveals a clear trade-off between reasoning gains and forgetting as the kernel shape shifts. The asymmetric kernel ($\alpha=1, \beta=2$) peaks at $p^* = 1/3$, tilting the curriculum toward harder problems; this yields the strongest MATH-500 score (95.4%, +1.4 over default) but increases forgetting to 0.9%. Pushing further to ($\alpha=1, \beta=3$) peaks at $p^* = 1/4$ and shows diminishing returns (94.9%) with sharply higher forgetting (2.4%), suggesting that weighting too-difficult problems eventually reintroduces the noisy-gradient problem the kernel is designed to avoid. In the opposite direction, kernels that peak at easier problems—($\alpha=2, \beta=1$) and ($\alpha=3, \beta=1$)—degrade MATH-500 to 91.5% and 90.3%, respectively, while also increasing forgetting (1.8% and 1.7%). This asymmetry corroborates the theoretical prediction: the student’s ZPD mean \bar{p}_Z lies below 0.5 on DAPO, so the optimal peak should lean toward harder problems. The default ($\alpha=\beta=1$) offers the best overall balance—strong reasoning improvement with near-zero forgetting (0.2%)—making it a robust default when the plasticity–stability trade-off matters.

4.3.2 Sensitivity to Number of Rollouts K

The pass-rate estimate $\hat{p}_i = (\# \text{ correct out of } K)$ controls the Beta kernel weights. We ablate $K \in \{4, 8, 16\}$ on Qwen3-8B distillation (forward KL, $\alpha=\beta=1$) to test (i) how estimation noise from

small K affects final performance, (ii) whether large K yields further gains, and (iii) the associated compute cost.

Table 7: Sensitivity to number of rollouts K for pass-rate estimation. All results use Qwen3-8B with forward KL and default exponents ($\alpha=\beta=1$). Rollout time is wall-clock for the single pass-rate estimation phase on $8\times H200$ GPUs.

K	MATH-500 (\uparrow)	AIME 24 (\uparrow)	AIME 25 (\uparrow)	MMLU Fgt. (\downarrow)
4	92.8%	40.1%	34.2%	0.2%
8	94.0%	41.6%	35.6%	0.2%
16	94.5%	42.5%	36.2%	0.3%

Interpretation. Halving the rollout budget to $K=4$ costs only 1.2 points on MATH-500 and 1.4 on AIME 25, while forgetting remains unchanged at 0.2%. This confirms that the Beta kernel’s smooth weighting is robust to the noisier pass-rate estimates from small K —unlike hard-threshold filters, a continuous weight function does not amplify estimation errors near the decision boundary. Doubling to $K=16$ yields marginal gains (+0.5 MATH-500, +0.6 AIME 25) with diminishing returns, suggesting $K=8$ strikes a practical balance between estimation quality and rollout cost. These results also quantify the compute overhead: the pass-rate estimation phase scales linearly in K , so $K=4$ halves the inference budget relative to $K=8$ with only modest accuracy loss, offering a useful knob when compute is constrained.

4.3.3 Why Forward KL for Distillation and Reverse KL for Self-Distillation

The Beta kernel controls *which* problems to train on; KL direction controls *how* probability mass is transferred.

- **Forward KL** ($\text{KL}(p_T \| p_S)$) is mode-covering. In the Qwen3 distillation setting, the larger teacher contains broader reasoning modes; forward KL encourages the smaller student to cover them rather than collapsing early.
- **Reverse KL** ($\text{KL}(p_S \| p_T)$) is mode-seeking. In the Qwen2.5 self-distillation setting, teacher and student are near-policy; reverse KL sharpens the student toward confident high-quality modes and stabilizes outputs.

To make this asymmetry explicit rather than only conceptual, we report a direct two-stage order comparison in Table 8. In this two-stage setting, pass rates are recomputed once between stages so that Stage 2 uses weights matched to the student’s updated competence after Stage 1.

Table 8: Two-stage order comparison on Qwen3 with the same pass-rate weighting $w(p) = p(1 - p)$. Pass rates are recomputed once between stages. Results are mean@8. The first two rows are single-loss references and the last two rows isolate schedule order.

Stage 1	Stage 2	MATH-500 (\uparrow)	AIME 24 (\uparrow)	AIME 25 (\uparrow)	MMLU Fgt. (\downarrow)
Paced KL	Paced KL	94.0%	41.6%	35.6%	0.2%
Paced RevKL	Paced RevKL	93.2%	40.9%	35.3%	0.1%
Paced RevKL	Paced KL	92.1%	38.9%	33.7%	0.3%
Paced KL	Paced RevKL	95.6%	43.9%	37.5%	0.1%

Takeaway. The order effect is large and consistent: KL \rightarrow RevKL improves over single-loss Paced KL by +1.6 (MATH-500), +2.3 (AIME 24), and +1.9 (AIME 25), while reversing the order (RevKL \rightarrow KL) underperforms both single-loss baselines. This directly supports the paper’s narrative: mode-covering first for exploration, then mode-seeking for consolidation.

This gives a natural bridge in the paper’s logic: first present cross-model distillation where coverage is the priority (forward KL), then present self-distillation where consolidation is the priority (reverse KL). In both cases, pass-rate weighting is identical and remains the common mechanism for selecting informative samples.

4.4 Deep Analysis (Validating Theory and Mechanisms: Gradients, Curriculum Evolution, etc.)

Pass-Rate Distribution. At initialization, roughly 17% of problems have $p < 0.2$ and 32% have $p > 0.8$, leaving about 51% in the productive middle range (Table 9). The $p(1-p)$ kernel recognizes this imbalance and responds accordingly, assigning near-zero weight to the crowded tails and concentrating training on the informative minority.

4.4.1 Curriculum Progression

Table 9 traces the migration of problems through the difficulty landscape during training using checkpointed pass-rate re-evaluation. As the student strengthens, problems flow steadily from the “too hard” regime ($p < 0.2$) through the zone of proximal development ($p \in [0.2, 0.8]$) and into the “mastered” side ($p > 0.8$): the fraction with $p > 0.8$ grows from 32% to 74% over 300 steps, while the average pass rate \bar{p} rises monotonically from 0.61 to 0.84. Notably, the Med- p bin shrinks from 51% to 21%, indicating that the pool of maximally informative problems is gradually depleted as the student masters more of the curriculum. This progressive depletion has a practical implication: the effective training signal weakens over time as fewer problems remain in the ZPD, which is consistent with the diminishing marginal returns typical of later training stages and naturally favors more consolidative objectives (e.g., reverse-KL behavior) once the ZPD has substantially contracted. The low- p tail also shrinks (from 17% to 5%), indicating that previously intractable problems gradually become tractable. This matters operationally in variants that recompute pass rates—such as our two-stage schedule, which re-estimates them once between stages—because newly accessible problems then receive larger weights after they enter the ZPD.

Table 9: Evolution of the pass-rate distribution and average pass rate \bar{p} across training. The distillation signal peaks when most problems enter the $p \in [0.2, 0.8]$ zone.

Training Stage	Low $p (< 0.2)$	Med $p (0.2-0.8)$	High $p (> 0.8)$	Avg pass rate \bar{p}
Step 0 (Init)	17%	51%	32%	0.61
Step 100	12%	32%	56%	0.70
Step 200	9%	24%	67%	0.78
Step 300	5%	21%	74%	0.84

4.4.2 Empirical Gradient SNR vs. Pass Rate

Figure 3 provides direct empirical validation of the theoretical SNR prediction. For each problem i , we sample $K=10$ rollouts and compute the distillation loss gradient with respect to the `lm_head` parameters for each rollout, yielding gradient vectors $g_i^{(1)}, \dots, g_i^{(K)}$. We then measure the per-problem SNR:

$$\widehat{\text{SNR}}_i = \frac{\|\bar{g}_i\|_2}{\sqrt{\frac{1}{K} \sum_{k=1}^K \|g_i^{(k)} - \bar{g}_i\|_2^2}}, \quad \bar{g}_i = \frac{1}{K} \sum_k g_i^{(k)}, \quad (8)$$

where the numerator measures the magnitude of the mean gradient (signal) and the denominator measures the spread across rollouts (noise). Since both are norms, $\widehat{\text{SNR}}_i \geq 0$. We then group problems into equal-width pass-rate bins and compute the mean $\widehat{\text{SNR}}$ within each bin; the bin means are rescaled to $[0, 1]$ by dividing by the largest bin mean. The bell-shaped profile predicted by Proposition 2 is clearly visible: SNR peaks at intermediate pass rates and is substantially lower at both boundaries, closely tracking the default $p(1-p)$ kernel.

5 Discussion: Limitations and Future Work

Several limitations deserve candid acknowledgment.

Rollout overhead. Pass-rate estimation requires K rollouts per problem per recomputation epoch. As discussed in Section 3.4, the cost is amortized across training steps and shared with reverse KL sampling; a two-phase screening strategy ($K_{\text{init}} \approx 4$) can further reduce inference by early-exiting on

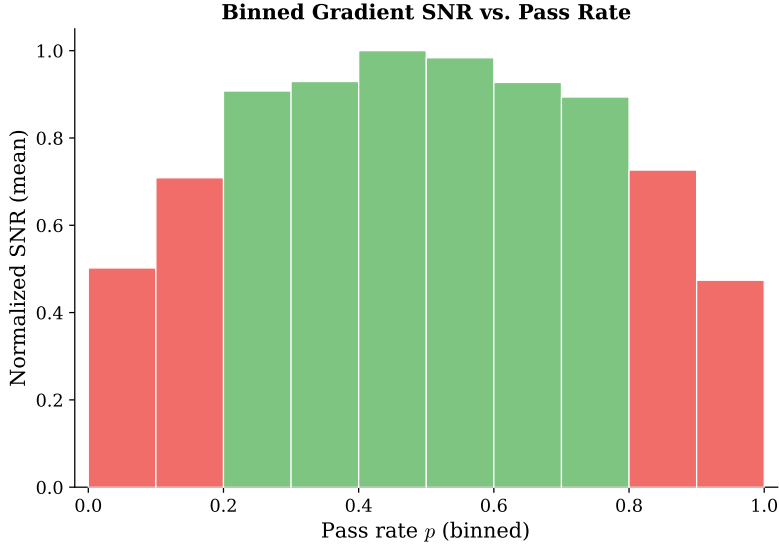


Figure 3: Empirical gradient SNR vs. student pass rate (Qwen3-8B, forward KL, $K=10$ rollouts). Gradients are computed at `lm_head`. Per-problem SNR values are averaged within each pass-rate bin; bin means are then normalized to $[0, 1]$ by dividing by the maximum bin mean. Red bars mark boundary regions ($p < 0.2$ or $p > 0.8$) where SNR is substantially lower; green bars mark the zone of proximal development where training signal is richest.

problems with $\hat{p} \in \{0, 1\}$. The Beta kernel’s smooth weighting is robust to noisy pass-rate estimates from moderate K (we use $K=8$), unlike hard filters that require precise thresholding.

Exponent selection. The closed-form method (Proposition 11) is a moment-matching heuristic; fully adaptive online estimation via gradient SNR tracking remains an open problem.

Future work. Several directions remain open. (i) *Continuous loss interpolation*: the two-stage schedule switches from forward KL to reverse KL at a fixed midpoint; a natural extension is continuous interpolation $\mathcal{L} = (1 - \lambda_t) \text{KL}_{\text{fwd}} + \lambda_t \text{KL}_{\text{rev}}$ with λ_t driven by ZPD statistics. (ii) *Cross-architecture and multi-teacher distillation*: pass-rate weighting is defined from student-side pass rates and may transfer naturally to cross-architecture settings (e.g., 70B \rightarrow 7B), where capacity mismatch pushes more problems into the $p \approx 0$ tail; multi-teacher ensembles—weighting each teacher–problem pair by student competence—are another natural extension.

6 Conclusion

A good teacher does not drill every problem with equal intensity—spending more time where a student struggles, moving past what is already mastered, and deferring what is still out of reach. PACED operationalizes this principle for LLM distillation: Beta-kernel pass-rate weighting (Eq. (3)) concentrates gradient budget on the frontier of a student’s competence while suppressing uninformative extremes. This weighting is not a design heuristic but a theoretical consequence—the Beta kernel family arises as a leading-order characterization of the boundary-vanishing structure of distillation gradients (Propositions 2–3), and is minimax-robust under bounded misspecification with worst-case efficiency loss $O(\delta^2)$ (Theorem 6). Empirically, in a split-track protocol (Qwen3 distillation with forward KL, Qwen2.5 self-distillation with reverse KL), PACED delivers substantial reasoning gains over corresponding baselines while incurring low retention loss, demonstrating that plasticity and stability need not be at odds. Because the weighting depends only on student rollouts, it is directly compatible with alternative objectives and training topologies; broader cross-architecture and multi-teacher validation remains future work.

References

- Rishabh Agarwal, Nino Vieillard, Yongchao Zhou, Piotr Stanczyk, Sabela Ramos, Matthieu Geist, and Olivier Bachem. On-policy distillation of language models: Learning from self-generated mistakes. *Proceedings of ICLR*, 2024.
- Jimmy Ba and Rich Caruana. Do deep nets really need to be deep? *NeurIPS*, 2014.
- Yoshua Bengio, Jérôme Louradour, Ronan Collobert, and Jason Weston. Curriculum learning. *ICML*, 2009.
- Nicolas Boizard, Kevin El Haddad, Céline Hudelot, and Pierre Colombo. Universal logit distillation. *arXiv preprint arXiv:2407.14053*, 2024.
- Mehrdad Farajtabar, Navid Azizan, Alex Mott, and Ang Li. Orthogonal gradient descent for continual learning. *AISTATS*, 2020.
- Robert M French. Catastrophic forgetting in connectionist networks. *Trends in Cognitive Sciences*, 3(4):128–135, 1999.
- Saeed Ghadimi and Guanghui Lan. Stochastic first- and zeroth-order methods for nonconvex stochastic programming. *SIAM Journal on Optimization*, 23(4):2341–2368, 2013.
- Alex Graves, Marc G Bellemare, Jacob Menick, Rémi Munos, and Koray Kavukcuoglu. Automated curriculum learning for neural networks. *ICML*, 2017.
- Yuxian Gu, Li Dong, Furu Wei, and Minlie Huang. MiniLLM: Knowledge distillation of large language models. *Proceedings of ICLR*, 2024.
- Dan Hendrycks, Collin Burns, Steven Basart, Andy Zou, Mantas Mazeika, Dawn Song, and Jacob Steinhardt. Measuring massive multitask language understanding. *Proceedings of ICLR*, 2021a.
- Dan Hendrycks, Collin Burns, Saurav Kadavath, Akul Arora, Steven Basart, Eric Tang, Dawn Song, and Jacob Steinhardt. Measuring mathematical problem solving with the MATH dataset. *NeurIPS*, 2021b.
- Geoffrey Hinton, Oriol Vinyals, and Jeff Dean. Distilling the knowledge in a neural network. *arXiv preprint arXiv:1503.02531*, 2015.
- Angelos Katharopoulos and François Fleuret. Not all samples are created equal: Deep learning with importance sampling. In *International Conference on Machine Learning (ICML)*, 2018.
- Taehyeon Kim, Jaehoon Oh, NakYoung Kim, Sangheum Cho, and Se-Young Yun. Comparing kullback-leibler divergence and mean squared error loss in knowledge distillation. *arXiv preprint arXiv:2105.08919*, 2021.
- Yoon Kim and Alexander M Rush. Sequence-level knowledge distillation. *Proceedings of EMNLP*, 2016.
- James Kirkpatrick, Razvan Pascanu, Neil Rabinowitz, Joel Veness, Guillaume Desjardins, Andrei A. Rusu, Kieran Milan, John Quan, Tiago Ramalho, Agnieszka Grabska-Barwinska, Demis Hassabis, Claudia Clopath, Dharshan Kumaran, and Raia Hadsell. Overcoming catastrophic forgetting in neural networks. *Proceedings of the National Academy of Sciences*, 114(13):3521–3526, 2017.
- M Pawan Kumar, Benjamin Packer, and Daphne Koller. Self-paced learning for latent variable models. *NeurIPS*, 2010.
- David Lopez-Paz and Marc’Aurelio Ranzato. Gradient episodic memory for continual learning. *NeurIPS*, 2017.
- OpenAI. gpt-oss-120b & gpt-oss-20b Model Card, 2025. URL <https://arxiv.org/abs/2508.10925>.
- Qwen Team. Qwen3 technical report. *arXiv preprint arXiv:2505.09388*, 2025.
- Mengye Ren, Wenyan Zeng, Bin Yang, and Raquel Urtasun. Learning to reweight examples for robust deep learning. In *International Conference on Machine Learning (ICML)*, 2018.
- Hejian Sang, Yuanda Xu, Zhengze Zhou, Ran He, Zhipeng Wang, and Jiachen Sun. On-policy self-distillation for reasoning compression. *arXiv preprint arXiv:2603.05433*, 2026.
- Idan Shenfeld, Mehul Damani, Jonas Hübner, and Pulkit Agrawal. Self-distillation fine-tuning. *arXiv preprint*, 2026.

- Naftali Tishby, Fernando C Pereira, and William Bialek. The information bottleneck method. *arXiv preprint physics/0004057*, 2000.
- Lev S Vygotsky. *Mind in Society: The Development of Higher Psychological Processes*. Harvard University Press, 1978.
- Wenhui Wang, Furu Wei, Li Dong, Hangbo Bao, Nan Yang, and Ming Zhou. Minilm: Deep self-attention distillation for task-agnostic compression of pre-trained transformers. In *Advances in Neural Information Processing Systems (NeurIPS)*, 2020.
- Taiqiang Wu, Chaofan Tao, Jiahao Wang, Runming Yang, Zhe Zhao, and Ngai Wong. Rethinking Kullback-Leibler divergence in knowledge distillation for large language models. In *Proceedings of the 31st International Conference on Computational Linguistics (COLING)*, pages 5737–5755, 2025.
- Yuanda Xu, Hejian Sang, Zhengze Zhou, Ran He, and Zhipeng Wang. Overconfident errors need stronger correction: Asymmetric confidence penalties for reinforcement learning. *arXiv preprint arXiv:2602.21420*, 2025.
- Shaotian Yan, Kaiyuan Liu, Chen Shen, Bing Wang, Sinan Fan, Jun Zhang, Yue Wu, Zheng Wang, and Jieping Ye. Distribution-aligned sequence distillation for superior long-cot reasoning. *arXiv preprint arXiv:2601.09088*, 2026.
- An Yang, Beichen Yang, Binyuan Hui, Bo Zheng, Bowen Yu, et al. Qwen2.5-math technical report: Toward mathematical expert model via self-improvement. *arXiv preprint arXiv:2409.12122*, 2024.
- Qiyang Yu, Zheng Zhang, Ruofei Zhu, Yufeng Yuan, Xiaochen Zuo, Yu Yue, Weinan Dai, Tiantian Fan, Gaohong Liu, Juncai Liu, Lingjun Liu, Xin Liu, Haibin Lin, Zhiqi Lin, Bole Ma, Guangming Sheng, Yuxuan Tong, Chi Zhang, Mofan Zhang, Ru Zhang, Wang Zhang, Hang Zhu, Jinhua Zhu, Jiase Chen, Jiangjie Chen, Chengyi Wang, Hongli Yu, Yuxuan Song, Xiangpeng Wei, Hao Zhou, Jingjing Liu, Wei-Ying Ma, Ya-Qin Zhang, Lin Yan, Mu Qiao, Yonghui Wu, and Mingxuan Wang. DAPO: An open-source llm reinforcement learning system. *arXiv preprint arXiv:2503.14476*, 2025.

A Complete Proofs

Proof roadmap. To keep the narrative intuitive while preserving logical rigor, we use the following dependency order:

1. Establish boundary conditions for distillation gradients (Proposition 2) and the boundary-to-Beta representation theorem (Proposition 3).
2. Use these structural results to obtain the non-monotonic learning-signal statement as a corollary-style consequence (Proposition 1).
3. Derive the descent-optimal weighting form and its robust minimax interpretation (Theorem 4, Theorem 6), then analyze variance and convergence.

A.0 Notation and Assumptions

Notation. Throughout the appendix, $p \in [0, 1]$ denotes the student pass rate for a problem, and $w(p) \geq 0$ denotes its pass-rate weight (typically a Beta kernel $w(p) = p^\alpha(1-p)^\beta$). We collect the shared assumptions here to avoid forward references in later proofs.

Symbol guide. Three distinct pairs of exponents appear in the analysis and should not be confused:

- (a_s, b_s) : *signal exponents*—govern how the expected gradient norm $\|\mathbb{E}[g(p)]\|$ scales with p near the boundaries (Assumption 3(a)).
- (a', b') : *SNR boundary exponents*—govern the power-law decay of $\text{SNR}^2(p)$ at $p \rightarrow 0^+$ and $p \rightarrow 1^-$ (Assumption 3(b)); these determine the shape of the theoretically optimal weight.
- (α, β) : *Beta kernel exponents*—the practitioner-facing hyperparameters in $w(p) = p^\alpha(1-p)^\beta$ (default $\alpha=\beta=1$).

Assumption 1 (Regularity Conditions). (i) The total loss $\mathcal{L}(\theta)$ is L -smooth; (ii) per-sample gradients are unbiased; (iii) per-sample gradient variance is bounded by σ_0^2 .

Assumption 2 (Bounded Logits and Jacobian). For all training steps and vocabulary dimensions v , the student and teacher logits are bounded as $|l_{S,v}|, |l_{T,v}| \leq B$, and the Jacobian of the student logits with respect to parameters satisfies $\|J_\theta\|_{op} = \|\partial l_S / \partial \theta\|_{op} \leq C_J$ for some constants $B, C_J > 0$.

Assumption 3 (Pass-Rate-Dependent Gradient Structure). The gradient statistics depend on pass rate p through:

- (a) Signal (Expected Gradient Norm): The expected gradient norm scales as $\|\mathbb{E}[g(p)]\| \propto p^{a_s}(1-p)^{b_s}$ for parameters $a_s, b_s > 0$, so the signal vanishes as $p \rightarrow 0$ (too hard) and $p \rightarrow 1$ (mastered).
- (b) SNR Boundary Vanishing and Power-Law Decay: The gradient SNR satisfies $\text{SNR}(p) \rightarrow 0$ as $p \rightarrow 0$ (a qualitative consequence of gradient incoherence; Proposition 2(ii) provides a sufficient condition) and exhibits asymptotic power-law boundary decay: $\text{SNR}^2(p)/p^{a'} \rightarrow c_0$ as $p \rightarrow 0^+$ and $\text{SNR}^2(p)/(1-p)^{b'} \rightarrow c_1$ as $p \rightarrow 1^-$ for some exponents $a', b' > 0$ and constants $c_0, c_1 \in (0, \infty)$. The power-law conditions imply $\text{SNR}(p) \rightarrow 0$ at both boundaries (at $p \rightarrow 1$, this follows from $b' > 0$; it is consistent with Proposition 2(i): $\|\mathbb{E}[g]\| \rightarrow 0$). This power-law regularity is an explicit structural modeling assumption used to obtain a closed-form leading term; it is not implied by smoothness alone. By Proposition 3, this yields the decomposition $\text{SNR}^2(p) = p^{a'}(1-p)^{b'} \cdot e^{r(p)}$ with bounded remainder r . The Beta kernel $p^{a'}(1-p)^{b'}$ is the leading-order (maximum-parsimony) approximation obtained by setting the shape variation of r to zero. When we write “ $\text{SNR}^2(p) \propto p^{a'}(1-p)^{b'}$ ” in subsequent results, this refers to this specialization; Theorem 6 provides a pointwise minimax statement and an aggregate lower bound for bounded r .
- (b') Weak SNR Condition (used for robustness analysis): A relaxation of (b): there exist $a', b' > 0$ and $\delta > 0$ such that $|\log(\text{SNR}^2(p)/(p^{a'}(1-p)^{b'}))| \leq \delta$ for all $p \in (0, 1)$. Equivalently, SNR^2 matches a Beta-family profile up to a bounded multiplicative perturbation $\phi(p) \in [e^{-\delta}, e^\delta]$, while ϕ is otherwise unrestricted (possibly non-monotone or multi-modal). Assumption (b) is the special case $\delta = 0$. For $\delta > 0$, the Beta kernel is no longer exactly

optimal for the exact saturated objective; Theorem 6 gives a pointwise minimax robustness statement for the first-order low-SNR model and a corresponding aggregate efficiency lower bound over \mathcal{F}_δ .

- (c) **Variance Profile at Extremes** (used only in examples): For some of our illustrative calculations (Proposition 10), we consider parameter regimes where the exponents $\gamma_1 = 2a_s - a'$ and $\gamma_2 = 2b_s - b'$ are negative, so that the gradient second moment $s^2(p) = \mathbb{E}[\|g(p)\|^2] \propto p^{\gamma_1}(1-p)^{\gamma_2}$ is larger near the boundaries than in the interior. This creates a natural anti-correlation between $s^2(p)$ (large at extreme pass rates) and Beta weights $w(p) = p^\alpha(1-p)^\beta$ (small at extremes), and will be used to exhibit concrete regimes where variance reduction occurs; it is not required for the general variance decomposition in Proposition 7 or for the basic convergence bound in Proposition 8.

Furthermore, the pass-rate distribution P is supported on $[\epsilon, 1 - \epsilon]$ for some $\epsilon > 0$, reflecting the granularity of finite rollouts ($\epsilon = 1/K$ with K rollouts). This ensures that all moments involving SNR^{-1} remain bounded.

Assumption 4 (Frozen Weights within Epochs (Adaptive Variant)). This assumption is used only for analyzing the optional adaptive variant with periodic pass-rate recomputation. Training is divided into epochs of T_0 gradient steps. At the beginning of each epoch, pass rates $\{p_i\}$ are recomputed and the Beta kernel weights $\{w(p_i)\}$ are updated accordingly. Within each epoch, the weights are held constant—that is, $w(p_i)$ does not depend on θ for the purpose of gradient computation. The convergence guarantee (Proposition 8) applies within each such epoch. The paper’s main experiments correspond to the single-pass special case where recomputation is disabled.

A.1 Non-Monotonicity of Learning Signal Quality (Motivating Corollary)

Definition 1 (Learning Signal Quality). For a problem x with student pass rate $p = p(x; \theta)$, define the learning signal quality as the expected information gain per gradient step:

$$Q(p) = \underbrace{\text{SNR}(g(x))}_{\text{gradient signal-to-noise}} \times \underbrace{(1-p)}_{\text{room for improvement}} \quad (9)$$

where $\text{SNR}(g(x))$ is the signal-to-noise ratio of the gradient computed on problem x .

Proposition 1 (Non-Monotonicity of Learning Signal). Under Assumption 3, together with the boundary and representation results in Propositions 2–3, the learning signal quality $Q(p)$ is non-monotone in p and peaks at intermediate pass rates: $Q(p) \rightarrow 0$ as $p \rightarrow 0$ (gradient variance dominates) and $Q(p) \rightarrow 0$ as $p \rightarrow 1$ (no room for improvement). The maximum occurs at some $p^* \in (0, 1)$ —the center of the zone of proximal development (Vygotsky, 1978).

Proof. Define $Q(p) = \text{SNR}(p) \cdot (1-p)$ where $\text{SNR}(g) = \|\mathbb{E}[g]\|_2 / \sqrt{\text{tr}(\text{Cov}(g))}$. The following boundary behavior and unimodality are formalized under Assumption 3.

The boundary behavior ($Q(0) = Q(1) = 0$) relies on the behavior of $\text{SNR}(p)$ near $p = 0$ and $p = 1$. We argue these limits hold based on the structure of distillation, then verify rigorously under Assumption 3.

Case $p \rightarrow 0$: The student assigns negligible probability to correct solutions. When $p \approx 0$, the student’s internal representations are poorly aligned with the target; conditioning on different minibatches of prompts at the same pass rate produces gradients whose directions vary widely ($\text{Cov}(g) \gg \|\mathbb{E}[g]\|^2$). The gradient direction depends on problem-specific discrepancies; when $p \approx 0$ the student’s predictions are near-random relative to y_T , so these discrepancies are dominated by noise rather than by a coherent learning signal, yielding $\text{SNR}(p) \rightarrow 0$ as $p \rightarrow 0$. (This boundary condition is established in Proposition 2(ii).)

Case $p \rightarrow 1$: The student already matches the target closely: $l_{S,t} \approx l_{T,t}$ and thus $\|\mathbb{E}[g]\| \rightarrow 0$. Moreover $(1-p) \rightarrow 0$. Note that $Q(p) = \text{SNR}(p)(1-p)$ is a $0 \cdot \infty$ -type product if $\text{tr}(\text{Cov}(g)) \rightarrow 0$ faster than $\|\mathbb{E}[g]\|^2$; hence $Q(p) \rightarrow 0$ is not automatic without a condition on $\text{SNR}(p)$ near $p = 1$. Under the leading-order representation (Proposition 3), $\text{SNR}^2(p) \sim p^{a'}(1-p)^{b'}$ with $b' > 0$, so $\text{SNR}(p) = \mathcal{O}((1-p)^{b'/2})$ and thus $Q(p) = \mathcal{O}((1-p)^{b'/2+1}) \rightarrow 0$ as $p \rightarrow 1$.

Existence of interior maximum. Since Q is continuous on $[0, 1]$ (inheriting continuity from the logit mapping), $Q(0) = Q(1) = 0$, and $Q(p) > 0$ for all $p \in (0, 1)$ (by Proposition 2(iii), $\text{SNR}(p) > 0$ for all $p \in (0, 1)$; combined with $(1 - p) > 0$, this gives $Q(p) > 0$), the extreme value theorem guarantees that Q attains its maximum at some $p^* \in (0, 1)$.

Remark on unimodality. The existence of a unique peak (unimodality) is not guaranteed by the above argument alone; Q could in principle have multiple local maxima. However, under the leading-order Beta representation (Proposition 3)—where $\text{SNR}^2(p) \sim p^{a'}(1 - p)^{b'}$ —the product $Q(p) = \text{SNR}(p) \cdot (1 - p) \propto p^{a'/2}(1 - p)^{b'/2+1}$ is indeed unimodal with a unique peak at $p^* = (a'/2)/((a'/2) + (b'/2 + 1))$. \square

A.2 Gradient Boundary Conditions and Representation Theorem

The following two propositions establish—under mild structural conditions on distillation—that the gradient learning signal degrades at both boundaries ($\text{SNR} \rightarrow 0$ at $p \rightarrow 0$; $\|\mathbb{E}[g]\| \rightarrow 0$ at $p \rightarrow 1$) and that any SNR profile with power-law boundary decay decomposes into a Beta leading term plus bounded remainder. These results, together with a power-law regularity condition (Assumption 3(b)), replace the need for a parametric assumption on the SNR profile.

Note: Proposition 1 (Section A.1) is included early for intuition. Its formal dependency follows the roadmap above: Assumptions \rightarrow Propositions 2–3 \rightarrow Proposition 1.

Proposition 2 (Gradient Boundary Conditions for Distillation). *Under Assumptions 1–2, for distillation with student pass rate p , suppose additionally:*

- (a) Alignment at mastery: $\mathbb{E}[\|l_S - l_T\|^2 \mid p] \rightarrow 0$ as $p \rightarrow 1$.
- (b) Gradient incoherence at incompetence: $\text{tr}(\text{Cov}(g(p)))/\|\mathbb{E}[g(p)]\|^2 \rightarrow \infty$ as $p \rightarrow 0$.

Then:

- (i) As $p \rightarrow 1$: $\|\mathbb{E}[g(p)]\| \rightarrow 0$ (gradient signal vanishes).
- (ii) As $p \rightarrow 0$: $\text{SNR}(p) \rightarrow 0$ (gradient noise dominates signal).
- (iii) $\text{SNR}(p) > 0$ for all $p \in (0, 1)$, and SNR is continuous on $(0, 1)$.

Conditions (a)–(b) are qualitative structural properties of distillation on diverse prompt sets—not parametric assumptions on the SNR profile. Intuitive justification is given in the proof. Consequently, the optimal weight $w^(p) \propto \text{SNR}^2(p)/(1 + \text{SNR}^2(p))$ satisfies $w^*(0) = 0$, $w^*(p) > 0$ for $p \in (0, 1)$, and the learning signal vanishes at $p \rightarrow 1$; the stronger conclusion $w^*(1) = 0$ follows from power-law regularity (Assumption 3(b)).*

Proof. Part (i). By condition (a), $\mathbb{E}[\|l_S - l_T\|^2 \mid p] \rightarrow 0$ as $p \rightarrow 1$. Since the softmax map is Lipschitz on $[-B, B]^V$ (Assumption 2), logit convergence implies $\mathbb{E}[\|p_S - p_T\|^2 \mid p] \rightarrow 0$. For KL-type losses the per-token gradient is $\nabla_{\theta} \mathcal{L}_t = J_{\theta}^{\top} (p_S - p_T)_t$ (or a similar linear-in-discrepancy form), so $\|\mathbb{E}[g(p)]\| \leq C_J \sum_t \mathbb{E}[\|p_{S,t} - p_{T,t}\|] \rightarrow 0$.

Justification of condition (a). In self-distillation (where teacher and student share the same architecture), $p \rightarrow 1$ means the student generates the correct solution with high probability. The teacher response y_T comes from the same model family; the student—which has learned to produce similar solutions—assigns high probability to each next token, implying convergence of the student’s predictions to the teacher’s. This argument is strongest for self-distillation with unambiguous targets; it may weaken for cross-architecture distillation where teacher and student use fundamentally different representations.

Part (ii). By condition (b), $\text{SNR}(p) = \|\mathbb{E}[g(p)]\|/\sqrt{\text{tr}(\text{Cov}(g(p)))} \rightarrow 0$ as $p \rightarrow 0$.

Justification of condition (b). When $p \rightarrow 0$, the student cannot produce the correct solution. The teacher response y_T contains reasoning the student has no internal representation for. Across different prompts with the same pass rate $p \approx 0$, the per-prompt gradient g_i has large norm but the mean $\mathbb{E}[g]$ over prompts is much smaller than a typical $\|g_i\|$: gradients from different intractable prompts interfere destructively. This gradient incoherence holds for *diverse* prompt sets (where $p \approx 0$

problems span many different skills); it would weaken for homogeneous problems sharing a common failure mode.

Part (iii). For $p \in (0, 1)$, the student has partial competence: $\|\mathbb{E}[g(p)]\| > 0$ (nonzero systematic logit discrepancy, since the teacher outperforms the student on average at pass rate $p < 1$) and $\text{tr}(\text{Cov}(g)) < \infty$ (bounded by σ_0^2 via Assumption 1(iii)), so $\text{SNR}(p) > 0$. Continuity follows from the continuous dependence of the logit mapping on (θ, x) .

Consequence. Since $h(x) = x/(1+x)$ is monotonically increasing with $h(0) = 0$, composing Part (ii) with $w^*(p) \propto \text{SNR}^2/(1+\text{SNR}^2)$ gives $w^*(0) = 0$ immediately. At $p \rightarrow 1$, Part (i) gives $\|\mathbb{E}[g]\| \rightarrow 0$; condition (a) also implies $\mathbb{E}[\|g\|^2] \rightarrow 0$, so the per-problem descent $\Delta(w^*, p) \rightarrow 0$ regardless of the weight value (the learning signal itself vanishes). The stronger conclusion $w^*(1) = 0$ holds when the SNR additionally exhibits power-law boundary decay (Assumption 3(b): $\text{SNR}^2(p) \sim c_1(1-p)^{b'} \rightarrow 0$). Combined with Part (iii), $w^*(p) > 0$ on $(0, 1)$ and w^* attains its maximum at some $p^* \in (0, 1)$. \square

Proposition 3 (Log-Linear Representation of Boundary-Vanishing Functions). *Let $f : (0, 1) \rightarrow \mathbb{R}_{>0}$ be continuous with $f(p) \rightarrow 0$ as $p \rightarrow 0^+$ and $p \rightarrow 1^-$. Suppose that f exhibits asymptotic power-law behavior at both boundaries: there exist exponents $\alpha_0, \beta_0 > 0$ and constants $c_0, c_1 \in (0, \infty)$ such that*

$$f(p)/p^{\alpha_0} \rightarrow c_0 \text{ as } p \rightarrow 0^+, \quad f(p)/(1-p)^{\beta_0} \rightarrow c_1 \text{ as } p \rightarrow 1^- \quad (10)$$

Then f admits the decomposition:

$$f(p) = p^{\alpha_0}(1-p)^{\beta_0} \cdot e^{r(p)} \quad (11)$$

where the remainder $r(p) = \log f(p) - \alpha_0 \log p - \beta_0 \log(1-p)$ converges to finite limits at both boundaries ($r(p) \rightarrow \log c_0$ as $p \rightarrow 0^+$; $r(p) \rightarrow \log c_1$ as $p \rightarrow 1^-$) and is bounded on $(0, 1)$: $\sup_p |r(p)| \leq \delta$ for some $\delta > 0$. The Beta kernel $p^{\alpha_0}(1-p)^{\beta_0}$ is the leading-order term: it captures the boundary decay rates exactly while introducing no shape modulation beyond the exponents (maximum parsimony).

Proof. The decomposition (11) holds by definition with $r(p) \triangleq \log f(p) - \alpha_0 \log p - \beta_0 \log(1-p)$. We verify that r is bounded.

Left boundary. By hypothesis, $f(p)/p^{\alpha_0} \rightarrow c_0$ as $p \rightarrow 0^+$, so $\log f(p) - \alpha_0 \log p \rightarrow \log c_0$. Since $\beta_0 \log(1-p) \rightarrow 0$ as $p \rightarrow 0^+$, we obtain $r(p) \rightarrow \log c_0$.

Right boundary. By hypothesis, $f(p)/(1-p)^{\beta_0} \rightarrow c_1$ as $p \rightarrow 1^-$, so $\log f(p) - \beta_0 \log(1-p) \rightarrow \log c_1$. Since $\alpha_0 \log p \rightarrow 0$ as $p \rightarrow 1^-$, we obtain $r(p) \rightarrow \log c_1$.

Since r is continuous on $(0, 1)$ (inheriting continuity from f) and converges to finite limits at both endpoints, it extends to a continuous function on $[0, 1]$ and is therefore bounded.

Why the stronger hypothesis is needed. The weaker condition $\lim_{p \rightarrow 0^+} \log f(p)/\log p = \alpha_0$ gives only $\log f(p) = \alpha_0 \log p + o(\log p)$, where $o(\log p)$ denotes a term growing slower than $|\log p| \rightarrow \infty$ —but not necessarily bounded. For example, $f(p) = p e^{\sqrt{|\log p|}}$ satisfies $\lim \log f/\log p = 1$ (so $\alpha_0 = 1$) but $r(p) = \sqrt{|\log p|} \rightarrow \infty$. The asymptotic power-law condition $f(p)/p^{\alpha_0} \rightarrow c_0$ is strictly stronger and ensures r converges to $\log c_0$ rather than diverging.

Maximum parsimony. Since w^* is defined only up to proportionality (the overall scale is absorbed by the learning rate), the constants c_0, c_1 are irrelevant for the weight profile. The Beta kernel $p^{\alpha_0}(1-p)^{\beta_0}$ is obtained by setting the *shape variation* of r to zero (i.e., $r \equiv \text{const}$), retaining only the boundary decay rates and no further structure—no bumps, oscillations, or interior asymmetries beyond what (α_0, β_0) prescribe. This is the information-theoretic sense of “maximum parsimony”: $\text{Beta}(\alpha_0+1, \beta_0+1)$ maximizes entropy among distributions on $[0, 1]$ with given expected sufficient statistics $(\mathbb{E}[\log p], \mathbb{E}[\log(1-p)])$. \square

A.3 Alternative Derivation: Per-Problem Descent Maximization

The structural characterization in Sections A.1–A.2 identifies the Beta kernel family directly from boundary conditions. Here we provide an independent, complementary derivation that arrives at the same family through gradient descent optimization—offering additional intuition for *why* the Beta kernel arises.

Definition 2 (Per-Step Guaranteed Descent Rate (Lower Bound on Descent)). For a problem x with pass rate p assigned weight $w(p) \geq 0$, the expected loss descent from a single gradient step with learning rate η satisfies the following lower bound (i.e., guaranteed minimum descent):

$$\Delta(w, p) = \eta w(p) \|\mathbb{E}[g(p)]\|^2 - \frac{\eta^2}{2} w(p)^2 \mathbb{E}[\|g(p)\|^2] \cdot \lambda_{\max}(\mathcal{H}) \quad (12)$$

where $g(p) = \nabla_{\theta} \mathcal{L}(\theta; x)$ is the per-sample gradient and \mathcal{H} is the loss Hessian. The second-order term uses $g^{\top} \mathcal{H} g \leq \lambda_{\max}(\mathcal{H}) \|g\|^2$, so $\Delta(w, p)$ is a lower bound on the true expected descent; the resulting w^* therefore maximizes the guaranteed descent rate rather than the exact descent.

Theorem 4 (Per-Problem Descent Maximization Yields Beta Kernel Weights). Consider the per-step descent lower bound $\Delta(w, p)$ in Definition 2. For each pass rate p , maximizing $\Delta(w, p)$ over $w(p) \geq 0$ yields the per-problem optimal weight $w^*(p) \propto \|\mathbb{E}[g(p)]\|^2 / \mathbb{E}[\|g(p)\|^2]$. Combined with boundary conditions on the gradient signal (Proposition 2) and power-law regularity (Assumption 3(b)), which together yield the log-linear representation $\text{SNR}^2(p) = p^{a'} (1-p)^{b'} \cdot e^{r(p)}$ with bounded r (Proposition 3), the per-problem optimal weight in the low-SNR regime takes the **Beta kernel form**:

$$w^*(p) = C \cdot p^{\alpha} (1-p)^{\beta} \quad (13)$$

where $(\alpha, \beta) = (a', b')$ and the peak occurs at $p^* = \alpha / (\alpha + \beta)$.

Proof of Theorem 4. Step 1: Pointwise optimization. Consider training on a single problem with pass rate p , so that $\mathcal{L}(\theta) = \mathcal{L}(\theta; x)$ and $g(p) = \nabla_{\theta} \mathcal{L}(\theta; x)$. A weighted gradient step $\theta \leftarrow \theta - \eta w(p) g(p)$ produces expected loss change (via Taylor expansion):

$$\mathbb{E}[\Delta \mathcal{L}] \approx -\eta w(p) \|\mathbb{E}[g(p)]\|^2 + \frac{\eta^2}{2} w(p)^2 \mathbb{E}[\|g(p)\|^2] \cdot \lambda_{\max}(\mathcal{H}) \quad (14)$$

Here the first-order term uses $\langle \mathbb{E}[g(p)], \nabla_{\theta} \mathcal{L} \rangle = \|\mathbb{E}[g(p)]\|^2$, which holds because the gradient estimator is unbiased for this per-sample loss. To maximize descent, differentiate with respect to $w(p)$ and set to zero:

$$-\eta \|\mathbb{E}[g]\|^2 + \eta^2 w^* \mathbb{E}[\|g\|^2] \lambda_{\max}(\mathcal{H}) = 0 \quad (15)$$

yielding:

$$w^*(p) = \frac{\|\mathbb{E}[g(p)]\|^2}{\eta \mathbb{E}[\|g(p)\|^2] \cdot \lambda_{\max}(\mathcal{H})} \propto \frac{\|\mathbb{E}[g(p)]\|^2}{\mathbb{E}[\|g(p)\|^2]} \quad (16)$$

Step 2: SNR decomposition. Using the bias-variance decomposition $\mathbb{E}[\|g\|^2] = \|\mathbb{E}[g]\|^2 + \text{tr}(\text{Cov}(g))$:

$$w^*(p) \propto \frac{\|\mathbb{E}[g]\|^2}{\|\mathbb{E}[g]\|^2 + \text{tr}(\text{Cov}(g))} = \frac{\text{SNR}^2}{1 + \text{SNR}^2} \quad (17)$$

Step 3: From SNR decomposition to Beta kernel via derived boundary conditions. From Step 2, $w^*(p) \propto \text{SNR}^2(p) / (1 + \text{SNR}^2(p))$. By Proposition 2, we have established that $\text{SNR}(p) \rightarrow 0$ as $p \rightarrow 0$ (gradient incoherence) and $\|\mathbb{E}[g(p)]\| \rightarrow 0$ as $p \rightarrow 1$ (alignment at mastery). Under the power-law regularity of Assumption 3(b), Proposition 3 yields the decomposition $\text{SNR}^2(p) = p^{a'} (1-p)^{b'} \cdot e^{r(p)}$ for boundary exponents $a', b' > 0$ and bounded remainder r . Setting $r \equiv 0$ —the maximum-parsimony approximation that retains only the derived boundary behavior—and substituting into Step 2, we proceed by regime analysis:

Low-SNR regime ($\text{SNR} \ll 1$, typical for distillation where per-sample gradient noise dominates):

$$w^*(p) \approx \text{SNR}^2(p) \approx p^{a'} (1-p)^{b'} \quad (18)$$

This yields the Beta kernel form with exponents $(\alpha, \beta) = (a', b')$.

High-SNR regime ($\text{SNR} \gg 1$): $w^*(p) \rightarrow 1$, assigning full weight. This regime corresponds to intermediate p where the student has both signal and capacity to learn.

General (mixed) regime: The exact optimal weight $w^*(p) = \text{SNR}^2 / (1 + \text{SNR}^2)$ is a saturating transformation of SNR^2 . Since $h(x) = x / (1 + x)$ is monotonically increasing with $h(0) = 0$, w^* inherits the qualitative properties from SNR^2 :

- *Zeros:* $w^*(0) = w^*(1) = 0$ (automatic filtering: $w^*(0) = 0$ from Proposition 2; $w^*(1) = 0$ from power-law decay, Assumption 3(b)).
- *Peak location:* $p^* = a'/(a' + b')$ (invariant to saturation).
- *Unimodal Beta-kernel profile:* The weight increases from $p = 0$ to p^* , then decreases to $p = 1$.

In the low-SNR regime the exponents are $(\alpha, \beta) = (a', b')$; the saturation in the mixed regime compresses these exponents. We therefore parameterize the weight as $w(p) = p^\alpha(1-p)^\beta$ with (α, β) as hyperparameters within the theoretically justified Beta kernel family:

$$w^*(p) \propto p^\alpha(1-p)^\beta, \quad p^* = \frac{\alpha}{\alpha + \beta} \quad (19)$$

The peak location p^* provides robust guidance for hyperparameter selection: the default $\alpha = \beta = 1$ yields the symmetric kernel $w(p) = p(1-p)$ with $p^* = 0.5$; asymmetric choices (e.g., $\alpha < \beta$ for emphasizing harder problems, or $\alpha > \beta$ for easier ones) shift the peak to $p^* = \alpha/(\alpha + \beta)$. The specific exponents are validated via ablation (Section 4.3).

Verification: $\partial^2 \Delta / \partial w^2 = -\eta^2 \mathbb{E}[\|g\|^2] \lambda_{\max}(\mathcal{H}) < 0$, confirming this is a maximum. □

Remark 1 (Per-Problem vs. Joint Optimization). *The derivation above optimizes $w(p)$ independently for each pass rate p , maximizing the per-problem descent guarantee. We discuss the relationship to joint (batch-level) optimization.*

Multi-sample descent structure. *In the multi-sample setting with batch gradient $\bar{g} = \frac{1}{N} \sum_i w_i g_i$, the expected descent is:*

$$\Delta_{batch} = \eta \left\| \frac{1}{N} \sum_i w_i \mu_i \right\|^2 - \frac{\eta^2 L}{2} \mathbb{E} \left[\left\| \frac{1}{N} \sum_i w_i g_i \right\|^2 \right] \quad (20)$$

where $\mu_i = \mathbb{E}[g_i]$. Even assuming gradient noise is uncorrelated across samples ($\text{Cov}(g_i - \mu_i, g_j - \mu_j) = 0$ for $i \neq j$), the objective still contains cross terms $\mu_i^\top \mu_j$ from both the signal term $\left\| \sum w_i \mu_i \right\|^2$ and the second-order term $\mathbb{E}[\left\| \sum w_i g_i \right\|^2]$. Additive decomposition into per-sample subproblems would require expected gradient orthogonality ($\mu_i^\top \mu_j = 0$ for $p_i \neq p_j$), which is a substantially stronger condition—and unlikely to hold in practice, since distillation gradients at different pass rates typically share significant directional overlap.

Normalization constraint. *The algorithm normalizes weights to unit mean ($\tilde{w}_i = w_i/\bar{w}$), introducing the constraint $\frac{1}{N} \sum_i \tilde{w}_i = 1$. However, this does not affect the optimal weight shape: the total gradient $\frac{1}{N} \sum_i \tilde{w}_i g_i = \frac{1}{N\bar{w}} \sum_i w_i g_i$ is equivalent to using unnormalized weights with a rescaled learning rate $\tilde{\eta} = \eta/\bar{w}$. The normalization therefore constrains only the effective learning rate, not the relative weighting profile.*

From per-problem to batch-level justification. *The per-problem analysis determines the weight shape through three complementary arguments: (a) the qualitative properties—boundary vanishing $w(0) = w(1) = 0$ and unimodal peak at $p^* = \alpha/(\alpha + \beta)$ —are determined by Propositions 2–3 and hold independently of the decomposition question; (b) Proposition 7 provides a separate, batch-level justification by showing Beta kernel weights reduce gradient variance under the variance-profile condition (Assumption 3(c)); (c) Assumption 4 decouples w from θ within each epoch, eliminating the dynamic coupling. Thus the Beta kernel form is supported by both per-problem descent maximization and batch-level variance reduction; the former pins down the functional form while the latter validates its effect in the multi-sample setting.*

Derivation path. *The Beta kernel form of w^* is derived rather than assumed: optimization gives $w^* \propto \text{SNR}^2/(1 + \text{SNR}^2)$, boundary conditions characterize the endpoint behavior, and Proposition 3 yields the Beta leading term with bounded remainder. For a compact end-to-end summary (including minimax robustness under misspecification), see Remark 3.*

A.4 Pointwise Minimax Robustness under Model Misspecification

The leading-order Beta kernel in Theorem 4 sets $r \equiv 0$ in the log-linear representation $\text{SNR}^2(p) = p^{a'}(1-p)^{b'} \cdot e^{r(p)}$ (Proposition 3). How robust is this choice when $r \neq 0$? Under the low-SNR

first-order approximation, we show that the Beta kernel is pointwise minimax-optimal over the uncertainty set $|r(p)| \leq \delta$, with a matching aggregate lower bound.

Lemma 5 (Quadratic Flatness of Descent Efficiency). *For any weight $w(p) \geq 0$ applied to a problem with true optimal weight $w^*(p)$, the descent efficiency ratio is:*

$$\frac{\Delta(w, p)}{\Delta(w^*, p)} = 2\rho - \rho^2 = 1 - (1 - \rho)^2 \quad (21)$$

where $\rho(p) = w(p)/w^*(p)$. In particular, a multiplicative misspecification $|\rho - 1| = \epsilon$ incurs only $O(\epsilon^2)$ efficiency loss.

Proof. From Definition 2, $\Delta(w, p) = \eta w \|\mathbb{E}[g]\|^2 - \frac{\eta^2}{2} w^2 \mathbb{E}[\|g\|^2] \lambda_{\max}(\mathcal{H})$. The optimal weight is $w^* = \|\mathbb{E}[g]\|^2 / (\eta \mathbb{E}[\|g\|^2] \lambda_{\max})$, yielding $\Delta(w^*) = \|\mathbb{E}[g]\|^4 / (2 \mathbb{E}[\|g\|^2] \lambda_{\max})$. Setting $w = \rho w^*$ and substituting:

$$\Delta(\rho w^*) = \eta \rho w^* \|\mathbb{E}[g]\|^2 - \frac{\eta^2}{2} \rho^2 (w^*)^2 \mathbb{E}[\|g\|^2] \lambda_{\max} = \Delta(w^*) (2\rho - \rho^2). \quad (22)$$

Since $2\rho - \rho^2 = 1 - (1 - \rho)^2$, the efficiency loss from $\rho \neq 1$ is exactly $(1 - \rho)^2$. \square

Theorem 6 (Pointwise Minimax Robustness of Beta Kernel in the Low-SNR Surrogate under Weak SNR Condition). *Consider the low-SNR regime where $w_\phi^*(p) \propto \text{SNR}^2(p) = p^{a'} (1 - p)^{b'}$ for an unknown perturbation ϕ satisfying $|\log \phi(p)| \leq \delta$ for all p (Assumption 3(b')). Define the uncertainty set $\mathcal{F}_\delta = \{\phi : (0, 1) \rightarrow \mathbb{R}_{>0} \mid |\log \phi(p)| \leq \delta \forall p\}$. Then:*

(i) *Under this first-order low-SNR approximation, the pointwise minimax-optimal weight is the **Beta kernel**:*

$$w_{\text{minimax}}(p) = \text{sech}(\delta) \cdot p^{a'} (1 - p)^{b'} \propto p^{a'} (1 - p)^{b'} \quad (23)$$

(ii) *Pointwise minimax efficiency: for every fixed $p \in (0, 1)$,*

$$\inf_{\phi(p) \in [e^{-\delta}, e^\delta]} \frac{\Delta_\phi(w_{\text{minimax}}, p)}{\Delta_\phi(w_\phi^*, p)} = \text{sech}^2(\delta) \geq 1 - \delta^2 \quad (24)$$

(iii) *Aggregate corollary: letting $R_\phi(p) = \Delta_\phi(w_{\text{minimax}}, p) / \Delta_\phi(w_\phi^*, p)$ and assuming $\Delta_\phi(w_\phi^*, p) \geq 0$ a.s.,*

$$\inf_{\phi \in \mathcal{F}_\delta} \frac{\mathbb{E}_P[\Delta_\phi(w_{\text{minimax}}, p)]}{\mathbb{E}_P[\Delta_\phi(w_\phi^*, p)]} \geq \text{sech}^2(\delta). \quad (25)$$

Proof. Step 1: Pointwise decomposition. Write the candidate weight as $w(p) = c(p) \cdot p^{a'} (1 - p)^{b'}$. The true optimal weight is $w_\phi^*(p) \propto p^{a'} (1 - p)^{b'} \phi(p)$, so $\rho(p) = c(p)/\phi(p)$. By Lemma 5, the per-problem efficiency is $f(\rho) = 2\rho - \rho^2$, which is strictly concave in ρ . The adversary (minimizer) selects $\phi \in \mathcal{F}_\delta$ to minimize $\mathbb{E}_P[f(c(p)/\phi(p))]$. Since $\phi(p)$ can be chosen independently at each p , the problem decomposes into per- p subproblems:

$$\max_{c(p) > 0} \min_{\phi(p) \in [e^{-\delta}, e^\delta]} f\left(\frac{c(p)}{\phi(p)}\right) \quad (26)$$

Step 2: Per- p minimax solution. At each p , the adversary pushes $\rho = c/\phi$ to the interval endpoints $\{ce^{-\delta}, ce^\delta\}$. The defender solves:

$$\max_{c > 0} \min\left(f(ce^\delta), f(ce^{-\delta})\right) \quad (27)$$

The minimax equalizer condition $f(ce^\delta) = f(ce^{-\delta})$ requires:

$$2ce^\delta - c^2e^{2\delta} = 2ce^{-\delta} - c^2e^{-2\delta} \quad (28)$$

$$c^* = \frac{1}{\cosh \delta} = \operatorname{sech}(\delta) \quad (29)$$

Crucially, c^* is independent of p , so $w_{\minimax}(p) = \operatorname{sech}(\delta) \cdot p^{a'}(1-p)^{b'} \propto p^{a'}(1-p)^{b'}$.

Step 3: Pointwise minimax efficiency value. Substituting $c^* = \operatorname{sech}(\delta)$ into $\rho_+ = c^*e^\delta = e^\delta / \cosh \delta$:

$$f(\rho_+) = 2\rho_+ - \rho_+^2 = \frac{2e^\delta}{\cosh \delta} - \frac{e^{2\delta}}{\cosh^2 \delta} = \frac{2e^\delta \cosh \delta - e^{2\delta}}{\cosh^2 \delta} = \frac{e^{2\delta} + 1 - e^{2\delta}}{\cosh^2 \delta} = \frac{1}{\cosh^2 \delta} = \operatorname{sech}^2(\delta) \quad (30)$$

where we used $2e^\delta \cosh \delta = e^{2\delta} + 1$. One verifies $f(\rho_-) = \operatorname{sech}^2(\delta)$ similarly, confirming the equalizer.

Since $\operatorname{sech}^2(\delta) = 1 - \tanh^2(\delta) \geq 1 - \delta^2$ (using $\tanh \delta \leq \delta$), the pointwise efficiency loss is at most δ^2 .

Step 4: Pointwise uniqueness and aggregate lower bound. Suppose $c(p_0) \neq \operatorname{sech}(\delta)$ at some p_0 with $P(p_0) > 0$. Then $\min(f(c(p_0)e^\delta), f(c(p_0)e^{-\delta})) < \operatorname{sech}^2(\delta)$ (since the per- p minimax is uniquely achieved by c^* , as follows from strict concavity of f). The adversary can exploit this at p_0 while playing the equalizer at all other points, yielding a strictly lower pointwise worst-case efficiency at that p_0 .

For the aggregate ratio, define $d_\phi(p) = \Delta_\phi(w_\phi^*, p) \geq 0$ and $R_\phi(p) = \Delta_\phi(w_{\minimax}, p) / \Delta_\phi(w_\phi^*, p)$. From Steps 2–3, $R_\phi(p) \geq \operatorname{sech}^2(\delta)$ pointwise in the worst case, so

$$\frac{\mathbb{E}_P[\Delta_\phi(w_{\minimax}, p)]}{\mathbb{E}_P[\Delta_\phi(w_\phi^*, p)]} = \frac{\mathbb{E}_P[R_\phi(p) d_\phi(p)]}{\mathbb{E}_P[d_\phi(p)]} \geq \inf_p R_\phi(p) \geq \operatorname{sech}^2(\delta), \quad (31)$$

which proves the aggregate lower bound in (iii). \square

Remark 2 (Quantitative Robustness of Beta Kernel). *The minimax efficiency $\operatorname{sech}^2(\delta)$ degrades gracefully with model misspecification:*

δ (log-scale uncertainty)	Multiplicative SNR ² range	Worst-case efficiency
0.1	[0.90, 1.11]	$\geq 99.0\%$
0.3	[0.74, 1.35]	$\geq 91.5\%$
0.5	[0.61, 1.65]	$\geq 78.6\%$
$\ln 2 \approx 0.69$	[0.50, 2.00]	$\geq 64.0\%$

Even when the true SNR² deviates from the Beta model by up to a factor of 2 ($\delta = \ln 2$), the Beta kernel retains at least 64% pointwise worst-case descent efficiency, and therefore at least this value as an aggregate lower bound under Theorem 6(iii). For moderate misspecification ($\delta \leq 0.3$, i.e., SNR² within 35% of the Beta model), this bound exceeds 91%.

Remark 3 (Summary: How the Beta Kernel Family Is Identified and Justified). *The Beta kernel $w(p) = p^\alpha(1-p)^\beta$ is derived, not assumed, through two independent lines of argument that converge on the same family:*

Primary argument (structural characterization + robustness):

1. Boundary conditions (Proposition 2): *In distillation, the gradient SNR vanishes at both boundaries—at $p \rightarrow 0$ due to gradient incoherence, at $p \rightarrow 1$ because $\|l_S - l_T\| \rightarrow 0$. These are structural properties of distillation, not parametric assumptions.*
2. Representation theorem (Proposition 3): *Under power-law boundary regularity (Assumption 3(b)), any such profile decomposes as $p^{a'}(1-p)^{b'} \cdot e^{r(p)}$ with bounded remainder r . The Beta kernel is the leading-order, maximum-parsimony term.*
3. Minimax robustness (Theorem 6): *Even when $r(p) \neq 0$, the Beta kernel remains minimax-optimal for the low-SNR leading-order objective over $\{|r| \leq \delta\}$, with only $O(\delta^2)$ efficiency loss, both pointwise and in aggregate.*

Alternative argument (gradient optimization, Appendix A.3): *Per-problem descent maximization independently yields $w^*(p) \propto \text{SNR}^2/(1 + \text{SNR}^2)$, which reduces to the same Beta kernel under the same boundary conditions. This provides complementary intuition: the Beta kernel maximizes the guaranteed descent rate for each problem.*

Both paths turn boundary-vanishing of distillation gradients into a concrete, robust weight family without circular reasoning. For RL-style training (binary correctness feedback with Bernoulli variance $p(1-p)$), the same boundary-vanishing intuition applies directly.

A.5 Convergence Analysis

We work under Assumptions 1–4, collected in Appendix A.0.

We denote by $\mathcal{L}_w(\theta) = \frac{1}{N\bar{w}} \sum_{i=1}^N w(p_i) \mathcal{L}(\theta; x_i)$ the Beta-kernel-weighted training loss (with $\bar{w} = \frac{1}{N} \sum_j w(p_j)$), and by \mathcal{L}_w^* its infimum.

A.5.1 Effective Gradient Variance

Proposition 7 (Effective Gradient Variance under Beta Kernel Weighting). *Consider the Beta-kernel-weighted gradient estimator for a uniformly sampled minibatch \mathcal{B} of size $|\mathcal{B}| = n$:*

$$\hat{g}_w(\theta) = \frac{1}{n\bar{w}} \sum_{i \in \mathcal{B}} w(p_i) g_i(\theta), \quad \tilde{w} = \frac{1}{N} \sum_{j=1}^N w(p_j) \quad (32)$$

where $w(p) = p^\alpha(1-p)^\beta$. Let $\tilde{w}(p) = w(p)/\bar{w}$ denote the normalized weight with $\mathbb{E}_P[\tilde{w}] = 1$. Define the (trace) variance of the weighted estimator by

$$\sigma_{\text{eff}}^2 \triangleq \frac{1}{n} \text{tr}(\text{Cov}_P(\tilde{w}g)) = \frac{1}{n} \left(\mathbb{E}_P[\tilde{w}^2 s^2] - \|\mathbb{E}_P[\tilde{w}g]\|^2 \right), \quad (33)$$

and the uniform baseline variance by $\sigma_{\text{unif}}^2 \triangleq \frac{1}{n} (\mathbb{E}_P[s^2] - \|\mathbb{E}_P[g]\|^2)$. The effective variance decomposes as:

$$\sigma_{\text{eff}}^2 = \frac{1}{n} \left(\underbrace{(1 + \text{Var}_P(\tilde{w})) \cdot \mathbb{E}_P[s^2]}_{\geq 1 \text{ (weight penalty)}} + \underbrace{\text{Cov}_P(\tilde{w}^2, s^2)}_{\text{weight-second-moment coupling}} - \|\mathbb{E}_P[\tilde{w}g]\|^2 \right) \quad (34)$$

where $s^2(p) = \mathbb{E}[\|g(p)\|^2]$ is the per-sample gradient second moment (including both signal and noise; see Remark in the proof). Non-uniform weighting always introduces a “weight penalty” term $(1 + \text{Var}_P(\tilde{w})) > 1$ (reflecting reduced effective sample size), together with a coupling term $\text{Cov}_P(\tilde{w}^2, s^2)$ and the mean-subtraction correction $\|\mathbb{E}_P[\tilde{w}g]\|^2$. As shown in the proof below, the variance ratio $R \triangleq \sigma_{\text{eff}}^2/\sigma_{\text{unif}}^2$ satisfies

$$R = \frac{1 + \text{Var}_P(\tilde{w}) + \frac{\text{Cov}_P(\tilde{w}^2, s^2)}{\mathbb{E}_P[s^2]} - \frac{\|\mathbb{E}_P[\tilde{w}g]\|^2}{\mathbb{E}_P[s^2]}}{1 - \frac{\|\mathbb{E}_P[g]\|^2}{\mathbb{E}_P[s^2]}}, \quad (35)$$

and, in particular, in the low-SNR regime where the mean terms are negligible relative to $\mathbb{E}_P[s^2]$, a sufficient condition for variance reduction simplifies to requiring the negative covariance term to overcome the weight penalty:

$$-\text{Cov}_P(\tilde{w}^2, s^2) > \text{Var}_P(\tilde{w}) \cdot \mathbb{E}_P[s^2]. \quad (36)$$

Assumption 3(c) describes parameter regimes where $s^2(p)$ is larger at the extremes than in the interior, which tends to make the covariance term negative; concrete examples where $R < 1$ for the default kernel are given in Proposition 10.

Proof. Eqs. (34)–(35) follow from the standard identity $\text{tr}(\text{Cov}(X)) = \mathbb{E}[\|X\|^2] - \|\mathbb{E}[X]\|^2$ applied to $X = \tilde{w}g$ (yielding the $\mathbb{E}_P[\tilde{w}^2 s^2]$ term via $\|\tilde{w}g\|^2 = \tilde{w}^2 \|g\|^2$), followed by the covariance decomposition $\mathbb{E}[UV] = \mathbb{E}[U]\mathbb{E}[V] + \text{Cov}(U, V)$ with $U = \tilde{w}^2$, $V = s^2$ and $\mathbb{E}_P[\tilde{w}^2] = 1 + \text{Var}_P(\tilde{w})$. Dividing numerator and denominator by $\mathbb{E}_P[s^2]$ gives Eq. (35); dropping the mean terms (negligible in the low-SNR regime) gives Eq. (36). Note that $s^2(p) = \|\mu(p)\|^2 + \text{tr}(\text{Cov}(g(p)))$ includes both

signal and noise; for teacher-forced distillation the gradient $g_i = \nabla_{\theta} \mathcal{L}(\theta; x_i)$ is deterministic given (θ, x_i) , so all stochasticity arises from minibatch sampling over prompts.

Example under the parametric model. Under Assumptions 3(a)–(b), $\|\mathbb{E}[g]\|^2 \propto p^{2a_s}(1-p)^{2b_s}$ and $\text{tr}(\text{Cov}(g)) = \|\mathbb{E}[g]\|^2 / \text{SNR}^2 \propto p^{2a_s - a'}(1-p)^{2b_s - b'}$; hence $s^2(p) = \mathbb{E}[\|g\|^2] = \|\mathbb{E}[g]\|^2 + \text{tr}(\text{Cov}(g))$ is a sum of two power-law terms. In the low-SNR regime (variance dominates: $\text{tr}(\text{Cov}(g)) \gg \|\mathbb{E}[g]\|^2$), we have $s^2(p) \propto p^{2a_s - a'}(1-p)^{2b_s - b'}$; alternatively, Assumption 3(c) posits this form directly. With $w(p) = p^{\alpha}(1-p)^{\beta}$, under Assumption 3(c) the exponents $\gamma_1 = 2a_s - a' < 0$ and $\gamma_2 = 2b_s - b' < 0$ ensure that $s^2(p) \rightarrow \infty$ as $p \rightarrow 0$ or $p \rightarrow 1$. Since $\tilde{w}(p)^2 \rightarrow 0$ at the same boundaries, the functions \tilde{w}^2 and s^2 are functionally anti-correlated: \tilde{w}^2 peaks at intermediate p while s^2 peaks at the boundaries.

For $p \sim \text{Uniform}[\epsilon, 1 - \epsilon]$ (approximating with $\epsilon \rightarrow 0$), the ratio R can be expressed via Beta-function moments:

$$R = \frac{B(2\alpha + \gamma_1 + 1, 2\beta + \gamma_2 + 1)}{B(\alpha + 1, \beta + 1)^2 \cdot B(\gamma_1 + 1, \gamma_2 + 1)} \quad (37)$$

where $B(\cdot, \cdot)$ denotes the Beta function. In the symmetric case ($\alpha = \beta = 1$, $a_s = b_s$, $a' = b' = 1$, so $\gamma = 2a_s - 1$), this simplifies to:

$$R(\gamma) = \frac{36(\gamma + 2)^2(\gamma + 1)^2}{(2\gamma + 5)(2\gamma + 4)(2\gamma + 3)(2\gamma + 2)} \quad (38)$$

Numerical evaluation: $R \approx 0.84$ for $a_s = 1/4$ ($\gamma = -1/2$); $R \approx 0.99$ for $a_s = 1/3$ ($\gamma = -1/3$); $R \approx 1.00$ for $a_s \approx 0.34$ (transition point); and $R > 1$ for $a_s \geq 1/2$ (no variance reduction). These calculations do *not* establish $R < 1$ for all parameter choices; they only exhibit concrete regimes under the parametric model where the low-SNR sufficient condition (36) holds (see also Proposition 10). In general, whether $R < 1$ should be checked via the exact ratio in Eq. (35); Eq. (36) is a convenient sufficient test only under the low-SNR approximation. \square

A.5.2 Convergence Rate

The following result is a standard application of the non-convex SGD convergence framework (see, e.g., Ghadimi and Lan (2013)); we state it here to make explicit how the effective variance σ_{eff}^2 from Proposition 7 enters the convergence bound.

Proposition 8 (Convergence Rate of Beta Kernel Weighted SGD). *Under Assumptions 1–4, SGD on the weighted objective \mathcal{L}_w with Beta-kernel-weighted gradients and learning rate η for T steps within a single recomputation epoch satisfies:*

$$\frac{1}{T} \sum_{t=0}^{T-1} \mathbb{E}[\|\nabla \mathcal{L}_w(\theta_t)\|^2] \leq \underbrace{\frac{2[\mathcal{L}_w(\theta_0) - \mathcal{L}_w^*]}{\eta T}}_{\text{optimization gap}} + \underbrace{\eta L \cdot \sigma_{\text{eff}}^2}_{\text{noise floor}} \quad (39)$$

where σ_{eff}^2 denotes the (trace) variance of the minibatch estimator under Beta-kernel reweighting (Proposition 7),

$$\sigma_{\text{eff}}^2 \triangleq \text{tr}(\text{Cov}(\hat{g}_w)) = \frac{1}{n} \left(\mathbb{E}_P[\tilde{w}^2 s^2] - \|\mathbb{E}_P[\tilde{w}g]\|^2 \right), \quad (40)$$

and the uniform baseline is $\sigma_{\text{unif}}^2 \triangleq \text{tr}(\text{Cov}(\hat{g}_{\text{unif}})) = \frac{1}{n} (\mathbb{E}_P[s^2] - \|\mathbb{E}_P[g]\|^2)$. Whether σ_{eff}^2 is smaller or larger than σ_{unif}^2 depends on the weight–variance coupling; when $\sigma_{\text{eff}}^2 < \sigma_{\text{unif}}^2$ the Beta kernel achieves a strictly lower noise floor than uniform SGD on \mathcal{L}_w .

Note: This theorem compares convergence on the weighted objective \mathcal{L}_w (which concentrates on intermediate-difficulty problems) versus uniform SGD on \mathcal{L}_w . It does not directly compare to uniform SGD on the unweighted objective $\mathcal{L}_{\text{unif}} = \frac{1}{N} \sum_i \mathcal{L}_i$; the exact variance comparison is given by Eq. (35), and in the low-SNR regime a convenient sufficient condition is Eq. (36) (see Proposition 10).

Proof of Proposition 8. Step 1: Per-step descent. By L -smoothness:

$$\mathcal{L}_w(\theta_{t+1}) \leq \mathcal{L}_w(\theta_t) - \eta \langle \nabla \mathcal{L}_w(\theta_t), \hat{g}_w(\theta_t) \rangle + \frac{L\eta^2}{2} \|\hat{g}_w(\theta_t)\|^2 \quad (41)$$

Step 2: Taking expectations. The expectation in Step 1 is over the minibatch at step t (conditional on θ_t). Using unbiasedness $\mathbb{E}[\hat{g}_w | \theta_t] = \nabla \mathcal{L}_w(\theta_t)$:

$$\mathbb{E}[\mathcal{L}_w(\theta_{t+1}) | \theta_t] \leq \mathcal{L}_w(\theta_t) - \eta \left(1 - \frac{L\eta}{2}\right) \|\nabla \mathcal{L}_w(\theta_t)\|^2 + \frac{L\eta^2}{2} \sigma_{\text{eff}}^2 \quad (42)$$

For $\eta \leq 1/L$, we have $1 - L\eta/2 \geq 1/2$. Taking full expectation over all minibatch draws up to t yields $\mathbb{E}[\mathcal{L}_w(\theta_{t+1})] \leq \mathbb{E}[\mathcal{L}_w(\theta_t)] - \frac{\eta}{2} \mathbb{E}[\|\nabla \mathcal{L}_w(\theta_t)\|^2] + \frac{L\eta^2}{2} \sigma_{\text{eff}}^2$.

Step 3: Telescoping. Summing from $t = 0$ to $T - 1$ and using the tower property, the sum telescopes:

$$\mathbb{E}[\mathcal{L}_w(\theta_T)] \leq \mathcal{L}_w(\theta_0) - \frac{\eta}{2} \sum_{t=0}^{T-1} \mathbb{E}[\|\nabla \mathcal{L}_w(\theta_t)\|^2] + \frac{L\eta^2 T}{2} \sigma_{\text{eff}}^2 \quad (43)$$

Rearranging and using $\mathcal{L}_w(\theta_T) \geq \mathcal{L}_w^*$:

$$\frac{1}{T} \sum_{t=0}^{T-1} \mathbb{E}[\|\nabla \mathcal{L}_w(\theta_t)\|^2] \leq \frac{2[\mathcal{L}_w(\theta_0) - \mathcal{L}_w^*]}{\eta T} + L\eta \sigma_{\text{eff}}^2 \quad (44)$$

Step 4: Noise floor comparison. The convergence bound in Step 3 holds for any σ_{eff}^2 as defined. When $\sigma_{\text{eff}}^2 < \sigma_{\text{unif}}^2$ (e.g., under Eq. (36) in the low-SNR regime, or in the examples of Proposition 10), choosing $\eta = O(1/\sqrt{T})$ yields:

$$T_{\text{beta}} = O\left(\frac{\sigma_{\text{eff}}^2}{\varepsilon^2}\right) \leq O\left(\frac{\sigma_{\text{unif}}^2}{\varepsilon^2}\right) = T_{\text{unif}} \quad (45)$$

Remark. The exact variance ratio is given by Eq. (35). In the low-SNR regime, Eq. (36) provides a convenient sufficient condition for $\sigma_{\text{eff}}^2 < \sigma_{\text{unif}}^2$, but it is not necessary outside that approximation. \square

Corollary 9 (Convergence Speedup). *If, in addition, $\sigma_{\text{eff}}^2 \leq \sigma_{\text{unif}}^2$ (e.g., verified via Eq. (35); in the low-SNR regime a sufficient condition is Eq. (36)), then achieving ε -stationarity on the weighted objective \mathcal{L}_w requires $T_{\text{beta}} = O(\sigma_{\text{eff}}^2/\varepsilon^2) \leq O(\sigma_{\text{unif}}^2/\varepsilon^2) = T_{\text{unif}}$ iterations, i.e., no slower (and possibly strictly faster) than uniform SGD on \mathcal{L}_w .*

A.5.3 Quantitative Variance Reduction

Proposition 10 (Quantitative Variance Reduction for Beta Kernels). *Under Assumptions 3(a)–(c) with the Beta kernel $w(p) = p^\alpha(1-p)^\beta$ and pass-rate distribution P supported on $[\varepsilon, 1-\varepsilon]$, the variance reduction ratio $R = \sigma_{\text{eff}}^2/\sigma_{\text{unif}}^2$ can be expressed in closed form via Beta-function moments (Eq. (37)). In the symmetric default case ($\alpha = \beta = 1$) with approximately uniform pass rates and moderate variance dominance ($a \approx 1/4$), this yields $R \approx 0.84$ (about $1.19\times$ reduction). For more strongly bimodal pass-rate distributions typical of early training (mass concentrated near $p \approx 0$ and $p \approx 1$), the boundary variance dominates while Beta weights vanish there, so R can be substantially below 1, indicating stronger variance reduction than in the uniform case.*

The derivations are straightforward but algebraically tedious and are omitted for brevity; we instead rely on these expressions to calibrate the expected magnitude of variance reduction in our experiments.

A.6 Data-Driven Exponent Selection

Theorem 4 establishes that the per-problem optimal weight lies in the Beta kernel family $w(p) = p^\alpha(1-p)^\beta$, but does not prescribe specific exponents. While the default $\alpha = \beta = 1$ is a robust choice, practitioners may benefit from adapting the kernel shape to the observed pass-rate distribution. We provide a principled, closed-form method for selecting (α^*, β^*) from data, requiring only the pass rates already computed for weighting.

Proposition 11 (Data-Driven Exponent Selection via Moment Matching). *Define the zone of proximal development (ZPD) as $\mathcal{Z} = \{i : \varepsilon \leq p_i \leq 1 - \varepsilon\}$ for cutoff $\varepsilon > 0$ (e.g., $\varepsilon = 1/K$), and let $P_{\mathcal{Z}}$ denote the restriction of the empirical pass-rate distribution P to \mathcal{Z} , with mean $\bar{p}_{\mathcal{Z}} = \mathbb{E}_{P_{\mathcal{Z}}}[p]$ and variance $v_{\mathcal{Z}} = \text{Var}_{P_{\mathcal{Z}}}(p)$.*

Since the kernel $w(p) = p^\alpha(1-p)^\beta$ normalized over $[0, 1]$ yields a $\text{Beta}(\alpha+1, \beta+1)$ density, the method-of-moments exponents (α^*, β^*) are obtained by fitting $\text{Beta}(\alpha+1, \beta+1)$ to the first two moments of $P_{\mathcal{Z}}$, i.e., $(\alpha+1)/(\alpha+\beta+2) = \bar{p}_{\mathcal{Z}}$ (normalized kernel mean = data mean) and $\text{Var}(\text{Beta}(\alpha+1, \beta+1)) = v_{\mathcal{Z}}$:

$$\frac{\alpha^* + 1}{\alpha^* + \beta^* + 2} = \bar{p}_{\mathcal{Z}}, \quad \alpha^* + \beta^* = \frac{\bar{p}_{\mathcal{Z}}(1 - \bar{p}_{\mathcal{Z}})}{v_{\mathcal{Z}}} - 3 \quad (46)$$

provided $v_{\mathcal{Z}} < \bar{p}_{\mathcal{Z}}(1 - \bar{p}_{\mathcal{Z}})/3$ (equivalently, $\alpha^* + \beta^* > 0$). Solving for individual exponents:

$$\alpha^* = \bar{p}_{\mathcal{Z}} \left(\frac{\bar{p}_{\mathcal{Z}}(1 - \bar{p}_{\mathcal{Z}})}{v_{\mathcal{Z}}} - 1 \right) - 1, \quad \beta^* = (1 - \bar{p}_{\mathcal{Z}}) \left(\frac{\bar{p}_{\mathcal{Z}}(1 - \bar{p}_{\mathcal{Z}})}{v_{\mathcal{Z}}} - 1 \right) - 1 \quad (47)$$

The kernel peak at $p^* = \alpha^*/(\alpha^* + \beta^*)$ is approximately $\bar{p}_{\mathcal{Z}}$ for concentrated distributions (large $\alpha^* + \beta^*$), ensuring the kernel focuses on informative samples. Moreover, the minimax robustness guarantee of Theorem 6 continues to hold for the data-driven exponents: if the true SNR profile satisfies Assumption 3(b') with the fitted (α^*, β^*) in place of (a', b') , then pointwise worst-case efficiency is at least $\text{sech}^2(\delta)$, with the same aggregate lower bound.

Proof. Step 1: Design rationale. Theorem 4 establishes that the per-problem optimal weight takes the Beta kernel form $w(p) = C p^\alpha(1-p)^\beta$ but does not specify the exponents (α, β) , which depend on the unknown SNR profile. A natural heuristic is to choose (α, β) so that the kernel concentrates its mass where the informative samples (those inside the ZPD) actually lie. This motivates matching the peak and spread of the kernel to the empirical distribution $P_{\mathcal{Z}}$ of pass rates within \mathcal{Z} .

Concretely, the kernel $w(p) = p^\alpha(1-p)^\beta$ normalized on $[0, 1]$ has integral $B(\alpha+1, \beta+1)$, so the corresponding probability density is $\text{Beta}(\alpha+1, \beta+1)$. We perform standard moment matching on this normalized kernel: let $a = \alpha+1$, $b = \beta+1$, and match the mean $a/(a+b) = \bar{p}_{\mathcal{Z}}$ and variance $ab/((a+b)^2(a+b+1)) = v_{\mathcal{Z}}$ of $\text{Beta}(a, b)$ to the data moments.

Step 2: Method-of-moments solution. With $a = \alpha + 1$, $b = \beta + 1$, we require:

$$\text{Mean matching: } \frac{a}{a+b} = \bar{p}_{\mathcal{Z}} \quad (48)$$

$$\text{Variance: } \frac{ab}{(a+b)^2(a+b+1)} = v_{\mathcal{Z}} \quad (49)$$

From Eq. (48): $b = a(1 - \bar{p}_{\mathcal{Z}})/\bar{p}_{\mathcal{Z}}$. Define $s = a + b$. Then $a = s\bar{p}_{\mathcal{Z}}$, $b = s(1 - \bar{p}_{\mathcal{Z}})$, and Eq. (49) gives:

$$\frac{s^2\bar{p}_{\mathcal{Z}}(1 - \bar{p}_{\mathcal{Z}})}{s^2(s+1)} = v_{\mathcal{Z}} \implies \frac{\bar{p}_{\mathcal{Z}}(1 - \bar{p}_{\mathcal{Z}})}{s+1} = v_{\mathcal{Z}} \implies s = \frac{\bar{p}_{\mathcal{Z}}(1 - \bar{p}_{\mathcal{Z}})}{v_{\mathcal{Z}}} - 1 \quad (50)$$

Converting back to kernel exponents: $\alpha^* = a - 1 = s\bar{p}_{\mathcal{Z}} - 1 = \bar{p}_{\mathcal{Z}} \left(\frac{\bar{p}_{\mathcal{Z}}(1 - \bar{p}_{\mathcal{Z}})}{v_{\mathcal{Z}}} - 1 \right) - 1$ and $\beta^* = b - 1 = s(1 - \bar{p}_{\mathcal{Z}}) - 1 = (1 - \bar{p}_{\mathcal{Z}}) \left(\frac{\bar{p}_{\mathcal{Z}}(1 - \bar{p}_{\mathcal{Z}})}{v_{\mathcal{Z}}} - 1 \right) - 1$, yielding Eqs. (46)–(47). The sum $\alpha^* + \beta^* = s - 2 = \bar{p}_{\mathcal{Z}}(1 - \bar{p}_{\mathcal{Z}})/v_{\mathcal{Z}} - 3$. The condition $\alpha^* + \beta^* > 0$ requires $v_{\mathcal{Z}} < \bar{p}_{\mathcal{Z}}(1 - \bar{p}_{\mathcal{Z}})/3$, i.e., the ZPD pass rates must be more concentrated than a uniform distribution ($v_{\text{Uniform}} = 1/12 = \bar{p}(1 - \bar{p})/3$ for $\bar{p} = 0.5$). When the data is exactly uniform, $s = 2$ and $\alpha^* = \beta^* = 0$, yielding the flat kernel $w(p) = 1$; the default $\alpha = \beta = 1$ reflects the theoretical prior from Theorem 4, not data adaptation.

Step 3: Robustness inheritance. Once (α^*, β^*) are selected, Theorem 6 applies directly with $(a', b') = (\alpha^*, \beta^*)$: if the true SNR profile is within a multiplicative $e^{\pm\delta}$ of $p^{\alpha^*}(1-p)^{\beta^*}$, pointwise worst-case efficiency is $\text{sech}^2(\delta) \geq 1 - \delta^2$, and the same value is an aggregate lower bound.

Remark (Boundary with the default). When the ZPD pass-rate distribution is symmetric ($\bar{p}_{\mathcal{Z}} = 0.5$) with variance $v_{\mathcal{Z}} = 1/12$ (approximately uniform on $[0, 1]$), we get $s = 0.25/(1/12) - 1 = 2$ and $\alpha^* = \beta^* = 0.5 \cdot 2 - 1 = 0$, yielding the flat kernel $w(p) = 1$. At $v_{\mathcal{Z}} = 1/20$ (more concentrated), the formula gives $s = 4$, $\alpha^* = \beta^* = 0.5 \cdot 4 - 1 = 1$, recovering the default $w(p) = p(1-p)$. Thus the data-driven MoM reduces to the theory-based default when the ZPD distribution is moderately concentrated, and relaxes to uniform weighting when the data lacks clear structure.

Remark (Practical interpretation). The formula has an intuitive reading:

- The *peak location* $p^* = \alpha^*/(\alpha^* + \beta^*) \approx \bar{p}_{\mathcal{Z}}$ (exact for $\bar{p}_{\mathcal{Z}} = 0.5$) says: focus training where most of the informative problems are.
- The *concentration* $\alpha^* + \beta^* = \bar{p}_{\mathcal{Z}}(1 - \bar{p}_{\mathcal{Z}})/v_{\mathcal{Z}} - 3$ says: if informative problems are tightly clustered (small $v_{\mathcal{Z}}$), use a peaked kernel; if they are spread out (large $v_{\mathcal{Z}}$), use a broad kernel.
- The *asymmetry* $\alpha^*/\beta^* \approx \bar{p}_{\mathcal{Z}}/(1 - \bar{p}_{\mathcal{Z}})$ (for large s) says: if the student struggles ($\bar{p}_{\mathcal{Z}} < 0.5$), emphasize harder problems ($\alpha < \beta$); if the student is mostly competent ($\bar{p}_{\mathcal{Z}} > 0.5$), emphasize consolidation ($\alpha > \beta$).

□

B Additional Connections and Interpretations

B.1 Additional Interpretations

The full pipeline can be viewed informally as a cascaded information bottleneck (Tishby et al., 2000):

$$Y_{\mathcal{E}} \xrightarrow{\text{reference generation}} Y_T \xrightarrow{\text{pass-rate weighting}} w(p) \cdot Y_T \xrightarrow{\text{distillation}} \theta_{\text{updated}}, \quad (51)$$

where (i) reference generation lets the teacher re-express expert solutions in its own distributional voice, (ii) pass-rate weighting down-weights problems with low learning signal via $w(p) = p^\alpha(1 - p)^\beta$, and (iii) distillation transfers knowledge from teacher to student via the chosen loss function. This view is purely interpretive and not used in our formal guarantees.

Remark 4 (Noise Filtering Interpretation). *At extreme pass rates, teacher-generated responses may carry teacher-specific artifacts, and $w(p) \rightarrow 0$ as $p \rightarrow 0$ or $p \rightarrow 1$ suppresses these noisy regimes. At intermediate pass rates, the student has sufficient capacity to extract transferable knowledge without memorizing artifacts, so $w(p) = p(1 - p)$ naturally focuses training on the student’s zone of proximal development, qualitatively resembling an information-bottleneck-style noise filter (Tishby et al., 2000).*

Remark 5 (Connection to Fisher Information). *The pass rate p can be viewed as the parameter of a Bernoulli random variable (correct/incorrect) with Fisher information $\mathcal{I}(p) = 1/(p(1 - p))$. The inverse Fisher information $p(1 - p)$ is exactly our default weight ($\alpha = \beta = 1$), and the generalization $p^\alpha(1 - p)^\beta$ allows asymmetric emphasis when practitioners wish to prioritize harder or easier problems.*

Remark 6 (Geometric Interpretation). *Let \mathcal{M}_θ denote the student’s representational manifold. For teacher responses at low pass rates, y_T is partially off-manifold and gradients contain orthogonal components that enable acquiring new capabilities; at high pass rates, y_T is nearly on-manifold and gradients are predominantly tangential, refining existing skills. The pass-rate kernel $w(p) = p(1 - p)$ scales both regimes, suppressing large off-manifold steps when $p \rightarrow 0$ and unnecessary tangential steps when $p \rightarrow 1$.*

C Hyperparameters

Hyperparameters. Table 10 summarizes the full configuration, which is shared across all models and method variants.

Parameter	Value
General	
Models	Qwen2.5-Math-7B-Instruct (self-distillation), Qwen3-8B (teacher: Qwen3-14B)
Data	
Training prompts	DAPO-Math-17k (Yu et al., 2025)
Max prompt length (student)	1,024 tokens (problem only)
Max prompt length (teacher)	3,072 tokens (problem + expert solution)
Max response length	16,384 tokens (training)
Generation (student rollout)	
Temperature	1.0
Rollouts per prompt (K)	8
Max generation tokens	8,192
Evaluation	
Benchmarks	MATH-500, AIME 2024, AIME 2025, MMLU
Metric	mean@8 accuracy (%)
Temperature	0.6
Top- p	0.95
Rollouts per prompt	8
Max generation tokens	30,000
Eval frequency	Every 10 steps
Training	
Optimizer	AdamW
Learning rate	1×10^{-7} (constant)
Weight decay	0.01
Gradient clipping	1.0 (max norm)
Global batch size	32
Micro-batch size per GPU	2
Epochs	1
Precision	bfloat16
Infrastructure	
GPUs	8 \times NVIDIA H200
Tensor parallelism (inference)	2
Sequence parallelism (training)	Ulysses, degree 8
FSDP parameter offload	Enabled
FSDP optimizer offload	Enabled
Gradient checkpointing	Enabled

Table 10: Hyperparameters for PACED. The same configuration is used across all models and method variants.